7048–7066 *Nucleic Acids Research, 2022, Vol. 50, No. 12* *Published online 23 June 2022*
https://doi.org/10.1093/nar/gkac499

PUMILIO competes with AUF1 to control DICER1 RNA levels and miRNA processing

Swetha Rajasekaran[1,2], Eshan Khan[1,2], Samuel R. Ching[3], Misbah Khan[1,2], Jalal K. Siddiqui[1,2], Daniela F. Gradia[4,5], Chenyu Lin[1,2], Stephanie J. Bouley[3], Dayna L. Mercadante[6], Amity L Manning[6,7], André P. Gerber[4], James A. Walker[3,8,9] and Wayne O. Miles[1,2,*]

[1]Department of Cancer Biology and Genetics, The Ohio State University, 460 West 12th Avenue, Columbus, OH 43210, USA, [2]The Ohio State University Comprehensive Cancer Center, The Ohio State University, 460 West 12th Avenue, Columbus, OH 43210, USA, [3]Center for Genomic Medicine, Massachusetts General Hospital, Boston, MA 02114, USA, [4]Department of Microbial Sciences, School of Biosciences and Medicine, Faculty of Health and Medical Sciences, University of Surrey, Guildford, Surrey GU2 7XH, UK, [5]Department of Genetics, Federal University of Parana, Curitiba, Brazil, [6]Bioinformatics and Computational Biology Program, Worcester Polytechnic Institute, 100 Institute Road, Worcester, MA 01609, USA, [7]Department of Biology and Biotechnology, Worcester Polytechnic Institute, 100 Institute Road, Worcester, MA 01609, USA, [8]Department of Neurology, Massachusetts General Hospital, Harvard Medical School, Boston, USA and [9]Cancer Program, Broad Institute of MIT and Harvard, Cambridge, MA 02142, USA

Received May 03, 2022; Editorial Decision May 18, 2022; Accepted May 27, 2022

ABSTRACT

DICER1 syndrome is a cancer pre-disposition disorder caused by mutations that disrupt the function of DICER1 in miRNA processing. Studying the molecular, cellular and oncogenic effects of these mutations can reveal novel mechanisms that control cell homeostasis and tumor biology. Here, we conduct the first analysis of pathogenic DICER1 syndrome allele from the DICER1 3′UTR. We find that the DICER1 syndrome allele, *rs1252940486*, abolishes interaction with the PUMILIO RNA binding protein with the DICER1 3′UTR, resulting in the degradation of the *DICER1* mRNA by AUF1. This single mutational event leads to diminished DICER1 mRNA and protein levels, and widespread reprogramming of miRNA networks. The in-depth characterization of the *rs1252940486* DICER1 allele, reveals important post-transcriptional regulatory events that control DICER1 levels.

INTRODUCTION

DICER1 is an RNA endoribonuclease that has a highly conserved role in the processing of mature miRNAs (1,2). The enzymatic activity of the RNase III domain of DICER1 cleaves a ∼70 nt precursor (pre) miRNAs into ∼22 nt mature miRNAs (1,3). These miRNAs are then assembled with the Argonaute (AGO) proteins as part of the RNA-Induced Silencing Complex (RISC) (4,5). Once incorporated into the RISC complex, miRNAs are utilized to regulate transcription (6), mRNA processing (7) and RNA fate (8). The most well characterized activity of miRNAs is in the post-transcriptional regulation of mRNAs (9,10). The RISC complex searches for sequences in mRNAs that are complementary to heptametric seed sequences within the miRNA (11,12). Once a match is identified, the RISC complex can trigger RNA cleavage and degradation (13,14), or inhibit mRNA translation (15,16).

Mature miRNA production is essential in both developmental and tumorigenic contexts, and alterations of miRNA levels have been shown to affect almost every cellular process (8,17–19). In cancer cells, widespread genomic and transcriptional changes alter miRNA levels (20) which contributes to tumor growth (21–26). OncomiRs are miRNAs that promote tumorigenic processes (17) and alterations in their levels enables carcinogenesis (27). Unsurprisingly, mutations that disrupt DICER1 function result in embryonic lethality (28) and severe phenotypic defects in adults (29–34). In addition, changes in DICER1 levels have been reported in many tumor types; however, how DICER1 contributes to tumorigenesis and patient outcome is context and dosage dependent (35). For example, reduced DICER1 levels correlate with shortened survival for patients with lung (36), gall bladder (37), colon (38) and ovarian cancers (39). In contrast, elevated DICER1 levels correlate with worse prognosis for patients with triple-negative

*To whom correspondence should be addressed. Tel: +1 614 366 2869; Email: wayne.miles@osumc.edu

breast cancer (TNBC) (40), prostate (41), esophageal (42) and colorectal cancers (43). These opposing clinical data highlight the importance of DICER1 regulation and suggest that DICER1 levels need to be maintained within a defined range, as both too much and too little DICER1 are prognostic in different tumors (44).

This rationale is supported by data from DICER1 syndrome, a cancer predisposition disorder caused by mutations of the *DICER1* gene (45). DICER1 syndrome patients are diagnosed with rare tumor types during early childhood (46,47) or adolescence (48,49). The bulk of DICER1 syndrome patients have mutations in the DICER1 coding sequence; specifically within critical residues of the RNase III domain that reduce or abolish miRNA processing (50,51). However, a number of mutations in DICER1 syndrome patients have been mapped outside of the DICER1 protein-coding region (52). The majority of these aberrations are located in the 3′ untranslated region (UTR) of DICER1, however the functional consequence of these mutations remains untested (53).

3′UTRs of mRNAs have important roles in regulating the stability, localization and protein translation of the transcript (54). Regulatory elements within the 3′UTR provide interaction sites for trans-regulatory factors including microRNAs or RNA-binding proteins (RBPs) that control RNA fate (55). The evolutionarily conserved Pumilio-FEM (PUF) family of RBPs, represented by the two paralogous proteins, PUMILIO1 (PUM1) and PUM2 in humans, act as key hubs within a large network of post-transcriptional regulators (56). This network of miRNAs and RBPs controls the fate and protein translation potential for almost every mRNA produced by cells (57). The human PUM proteins bind with high affinity to a conserved PUMILIO Regulatory Element (PRE) (5′-UGUAHAUA-3′, where H = A, U or C), which are predominantly found in the 3′UTRs of mRNAs (58,59). In conjunction with other mRNA regulatory factors, the PUM proteins cooperate and/or compete to bind and regulate their substrates (60). PUM homologs have been identified in all eukaryotes and are highly conserved amongst species (61,62). The PUM proteins have important roles in regulating an array of biological processes including cell cycle (59,63–65), pluripotency (66,67), differentiation (68–70), metabolism (71,72), immune response (73,74) and apoptosis (66,75). Mutations within the PUM proteins or their dysregulation result in various pathological conditions, including stem cell exhaustion (66,76), cancer (63,64,77), ataxia (78,79), epilepsy (80,81) and infertility (66,82). The PUM proteins have context and tissue-specific roles in regulating mRNA and can alter RNA fate using multiple mechanisms, including 5′-decapping (83), ribosome stalling (84), de-adenylation (85) and facilitating miRNA recruitment (63,64). By utilizing these processes, the PUM proteins act as key regulators of mRNA and can either promote or suppress the protein translation of their substrates (57).

To identify post-transcriptional mechanisms regulating DICER1 levels, we search the 3′UTR of DICER1 for regulatory elements, and found two highly conserved PREs. We then tested whether the PUM proteins regulate DICER1 and found that PUM was required for DICER1 RNA stability, protein levels and mature miRNA production. Highlighting the importance of this regulation, we found two clustered mutations (*rs1252940486 A > G*, *rs1291805809 A > C*) in DICER1 syndrome patients that disrupted the distal PRE within the *DICER1* gene. We then tested these mutations and found reduced PUM-DICER1 RNA interaction, lower DICER1 and miRNA levels. Utilizing CRISPR-Cas9 knock-ins and RNA-RBP purifications, Mass Spectrometry, and mechanistic studies, we show that PUM binding to the *DICER1* mRNA competes and protects it from the activity of the AUF1 RBP and that mutations that diminish the interaction of PUM1, enable AUF1 binding. Our in-depth analysis of DICER1 regulation highlights the importance of PUM-mediated regulation of DICER1.

MATERIALS AND METHODS

Cell lines

MDA-MB-231, RPE1, HEK 293T, DLD1 and HCT116 cell lines were obtained from ATCC (#HTB-26, #CRL-4000, #ACS-4500, #CCL-221, #CCL-247) and confirmed by STR profiling. MDA-MB-231, RPE1 and HEK 293T cell lines were cultured in Dulbecco's modified essential medium—high glucose (DMEM-high glucose, Invitrogen) supplemented with 10% fetal bovine serum, L-glutamine and 1× penicillin–streptomycin solution as specified by ATCC regulation. DLD1 cell line was cultured in RPMI-1640 supplemented with 10% fetal bovine serum, L-glutamine and 1× penicillin-streptomycin solution as specified by ATCC regulation. HCT116 cells were maintained in McCoy's 5A (modified) media and supplemented with 10% fetal bovine serum, L-glutamine and 1× penicillin–streptomycin solution as specified by ATCC regulation. The cells were maintained in a humidified 37°C incubator with 5% CO_2. The cells were routinely tested for mycoplasma contamination.

Plasmids

For Luciferase assay, DNA oligos containing WT 3′UTR and pMUT sequences were cloned into psicheck2 plasmid digested with XhoI restriction enzymes. The cloning reaction was performed using Gibson Assembly according to manufacturer's protocol. Samples were then incubated in a thermal cycler at 50°C for 15 min, and transformed into NEB 5-alpha competent cells for further propagation. The plasmids were cultured in LB media and mini prepped using Qiagen miniprep kit for transfection into mammalian cell lines.

For DICER1 3′UTR WT fragment, the sequence was obtained from pIS-DICER1 which was purchased from Addgene. The sequences were PCR amplified with the sticky ends of the restriction enzyme on the 5′ end and 3′end of the fragment. The psicheck2 luciferase reporter plasmid was digested with XhoI and NotI restriction enzyme and the purified DNA amplicons were cloned using ligation. To mutate the first PRE (A mut), second PRE (B mut) and both PREs (AB mut), QuikChange II Site-Directed Mutagenesis kit protocol was used as per manufacturer instructions. Briefly, primers were designed with the appropriate

mutations (TGTAAATA > TCCAAATA) using the Agilent primer design website (https://www.agilent.com/store/primerDesignProgram.jsp). The PCR reaction was set up as specified by the protocol as follows: 95°C (30 s) 1 cycle; 95°C (30 s), 55°C (1 min), 68°C (1 min/kb plasmid) 15 cycles. Following this reaction, the samples were treated with DpnI restriction enzyme and transform into competent cells. The plasmids were cultured in LB media and mini prepped using Qiagen miniprep kit for transfection into mammalian cell lines.

Sequences coding for the C-terminal tandem affinity purification (TAP)-tag were amplified with primers TAP1-NotIFw and TAP2-XhoIRev from plasmid pBS1479 (86) by PCR and cloned into pcDNA3.1 (Invitrogen) via NotI and XhoI restriction sites, generating plasmid pcDNA3.1-TAP. The sequences encoding the CDS of Pum1 and PUM2 were PCR amplified from cDNA clones IRAUp969B1150D (PUM1) and IRAUp969G0177D (PUM2) from the Deutsches Ressourcenzentrum für Genomforschung (RZPD) with primer pairs: PUM1-FL-EcoRVFwd/ PUM1-HD-NotIRev, and PUM2-HD-EcoRVFwd/PUM2-HD-NotIRev, and cloned via EcoRV and NotI sites into pcDNA3.1-TAP, producing the plasmids pcDNA3.1-PUM1-FL-TAP, and pcDNA3.1-PUM2-HD-TAP, respectively.

pDEST-HA-PUM1 and PUM2 were previously generated by our group and the details of its constructed are outlined in the following publication (64).

Transfections

For luciferase assays, 5×10^4 cells were seeded in each well of a 24-well plate 24 h before transfection. The next day, the luciferase plasmids were transfected using LipoLTX (Thermo Fisher) using manufacturer protocol. Fresh medium was provided the next morning and the cells were incubated at 37°C with 5% CO_2 in a humidified incubator. The transfected cells were then lysed using passive lysis buffer provided in the Dual Luciferase Assay kit (Promega).

For luciferase assays under PUM depletion, the cells were first infected with lentiviral vectors with sh-SCR or sh-PUM1/sh-PUM2. We used two shRNAs was each target with each vector targeting a different region on the transcript. The cells were then allowed to recover and selected in the appropriate selection media. After selection, 5×10^4 cells were then seeded in each well of a 24-well plate 24 h before transfection. The plasmids were transfected as mentioned above and the cells were lysed using passive lysis buffer provided in the Dual Luciferase Assay kit (Promega).

For luciferase assays with PUM protein overexpression, 5×10^4 cells were seeded in each well of a 24-well plate 24 h before transfection. The next day, the luciferase plasmids were co-transfected with pDEST-PUM1, pDEST-PUM2 or pcDNA-empty vector using manufacturer protocol for LipoLTX (Thermo Fisher). The transfected cells were then lysed using passive lysis buffer provided in the Dual Luciferase Assay kit (Promega).

For PUM1-TAP overexpression, HEK-293T cells were seeded at 50% confluency 24 h prior to transfection. The next day, the cells were transfected with pcDNA3.1-PUM-FL-TAP plasmids using Lipo2000 (Thermo Fisher) with manufacturer protocol. The media was changed after 4 h and cells were incubated at 37°C with 5% CO_2 in a humidified incubator. The cells were then lysed in polysome lysis buffer (10 mM HEPES (pH 7.0), 100 mM KCl, 5 mM $MgCl_2$, 25 mM EDTA (pH 8), and 0.5% NP40. Prior to use, the following components were added per 50 ml of PLB buffer: one tablet of complete proteinase inhibitor (Roche), 2 mM DTT, 50 U/ml RNase OUT (Sigma) and heparin 0.2 mg/ml) 48 h after transfection and the lysates were tested using western blot before use in *in vitro* binding assays.

For PUM1 and PUM2 overexpression studies, 2×10^5 cells were seeded on each well of a six-well plate 24 h before transfection. The cells were then transfected with 2 μg of pcDNA-empty vector, or increasing amounts of pcDNA-HA-PUM1 plasmid using Lipo2000 (Thermo Fisher) with manufacturer protocol. Fresh media was provided after 4 h and the cells were incubated at 37°C with 5% CO_2 in a humidified incubator. The cells were then lysed for western blots using RIPA lysis buffer 48 h after transfection.

Lentiviral vector packaging and delivery

DNA of lentiviral plasmids (sh-PUM1: TRCN0000147347, TRCN0000146945; sh-PUM2: TRCN0000061859, TRCN0000061861; sh-AUF1: TRCN0000293283, TRCN0000293353; sh-LARP4: TRCN0000160140, TRCN0000164286; sh-STAU2: TRCN0000102356, TRCN0000102357; sh-laAUF1: TRCN0000236572, TRCN0000236575; pLenti-puro-luciferase) were prepared using Qiagen midiprep kit. The virus was packaged in HEK 293T cells using the Takara Lenti-X Single Shot kit according to manufacturer's instruction. The lentivirus was then filtered and concentrated 10X using PEG-NaCl solution. 5×10^4 cells were seeded in each well of a 24-well plate 24 h before infection and the cells were infected in media containing 0.8 μg/ml final concentration of polybrene and spun at 2000 rpm, 1 h at room temperature before being incubated in a humidified 5% CO_2 incubator overnight at 37°C. The next morning, the infected cells were provided with fresh media and allowed to recover for 24 h. Puromycin selection (1.5 μg/ml for MDA-MB-231) was performed for 2 days and cells were lysed for further analysis.

Western blots

Protein samples were prepared by lysing cells or xenograft tumors in 4% SDS buffer and sonicating 10 s on, 20 s off, 5 cycles at 4°C. The protein lysate (30 μg) were mixed with 3× loading buffer (CST) and denatured at 95°C for 5 min. These protein samples were then loaded on a SDS-PAGE gel under denaturing condition at 120 V for 90 min at RT in Tris-Glycine-SDS running buffer. The proteins were then transferred on to a PVDF membrane (Biorad) using predefined protocol for mixed molecular weight proteins. The membrane was blocked using 10% non-fat milk and washed with TBST buffer. After washing, the membrane was incubated with the corresponding primary antibodies diluted in 5% non-fat milk and TBST overnight at 4°C with gentle shaking. The membranes were then washed 3 times with

TBST buffer for 10 min each at RT and then probed with the corresponding HRP-conjugated secondary antibody for 2 h at RT. After this incubation, the membrane was washed with TBST buffer 3× for 10 min each at room temperature and the protein were detected using Amersham ECL prime western blotting detection reagent (Amersham) following manufacturer's instructions. The membrane was imaged using LiCor image analyzer under ECL conditions and ImageStudio software is used for further analysis. Beta-Actin is used as a loading control for the western blot experiments and all blots shown here is a representative mean image of at least three experimental replicates.

Antibodies

PAP antibody (Sigma #P1291)—antibody dilution 1:1000; DICER1 (CST #3363S)—primary antibody dilution 1:500, secondary antibody dilution 1:1000; HA antibody (CST #3724)—primary antibody dilution 1:1000, secondary antibody dilution 1:2000, PUM1 (Abcam #ab92545)—primary antibody dilution 1:1000, secondary antibody dilution 1:1000; PUM2 (R&D #MAB7415)—primary antibody dilution 1:500, secondary antibody dilution 1:1000; AUF1 (CST #12382)—primary antibody dilution 1:1000, secondary antibody dilution 1:2000; LARP4 (Fisher #50-156-6366)—primary antibody dilution 1:1000, secondary antibody dilution 1:1000; STAU2 (Santa Cruz #sc-101144)—primary antibody dilution 1:1000, secondary antibody dilution 1:1000; laAUF1 (Abcam #ab83215)—primary antibody dilution 1:1000, secondary antibody dilution 1:1000; β-actin (CST #3700)—primary antibody dilution 1:5000, secondary antibody dilution 1:5000. The appropriate secondary antibodies were used for western blot analysis—anti-mouse HRP (Fisher #45000679), anti-rabbit HRP (Fisher #45000682).

RT-PCR analysis

RNA was isolated from each well using Qiagen RNeasy kit according to manufacturer's instructions and cDNA was prepared from 250 ng of RNA using the High Capacity cDNA Reverse Transcription kit (Applied Biosystems) according to manufacturer's protocol. The expression of specific target genes was quantified by quantitative PCR using Fast Start Universal SYBR Green Master with ROX (Roche) and was normalized to the expression of β-actin (cDNA dilution = 1:10) and the control samples. See Primer section for sequence. All q-RT-PCR experiments were performed using Roche SYBR green master mix under the following cycling conditions: initial denaturation—95 C (10 min); 95 C (15 s), 60 C (1 min) for 40 cycles; 95 C (15 s), 60 C (1 min), 95 C (15 s) for melt curve

Luciferase assay

The corresponding 3′UTR sequences were cloned into psiCheck2 vector (Promega) with Renilla Luciferase as the reporter and an internal Firefly Luciferase control. The cell lines were transfected with Lipofectamine2000 (Thermo) according to manufacturer's protocol and were lysed 48 h after transfection in passive lysis buffer from the Promega Dual Luciferase Kit. Luciferase assays were performed using Promega Dual Luciferase Kit with passive lysis for 15 min followed by addition of LAR II substrate and StopN-Glo with luminometer readings between the two substrates.

Synthesis of biotinylated RNAs and RNA pull-down experiments

DNA templates for the 3′UTR region of DICER1 that contains the two PREs (PRE1: 3876–3975, PRE2: 3975–4076) were synthesized from Sigma bearing a T7 RNA polymerase promoter sequence at the 5′ end of the oligo. The DNA templates for the PRE mutation containing sequences were prepared using the method described above but from previously constructed plasmids using Quikchange. DNA templates for the DICER's 3′UTR region that contains the two PRE (from nucleotides 9785–10276) for biotin-RNA synthesis were prepared by PCR from human DNA with oligonucleotides bearing a T7 RNA polymerase promoter sequence at the 5′ end of the forward primer (3′ UTR DICER PRE Fwd/ 3′UTR DICER Rv). As controls, biotinylated RNAs from 3′UTR of VEGFA (3′UTR VEGFA-T7 Fwd /′UTR VEGFA Rv 3′) and from 3′UTR of MRAS (3′UTR MRAS-T7 Fwd/3′UTR MRAS Rv) were also prepared.

The PCR fragments were gel purified (Qiagen) and the RNA bait was transcribed *in vitro* and biotinylated using T7 polymerase (Sigma) and Roche Biotinylation mix (Sigma). The biotinylated RNA (1 μg) was incubated with 150 μg cell lysate (HEK 293T overexpressing TAP-PUM1) for 30 min at RT with rotation in binding buffer (10 mM HEPES–KOH (pH 7.5), 100 mM KCl, 5 mM $MgCl_2$, 25 mM EDTA, 0.5% IGEPAL, 2 mM DTT, 0.2 mg/ml, 1 mg/ml yeast tRNA and 1× protease inhibitor). The mixture was then incubated with magnetic streptavidin beads (Fisher) for 30 min, with spinning at RT. The beads were washed 4× in wash buffer (50 mM Tris–HCl (pH 7.5), 300 mM NaCl, 1 mM EDTA, 1% IGEPAL, 0.1% SDS, 0.5% Na-deoxycholate, 1× protease inhibitor) and the protein bound to the beads were eluted using RIPA buffer and incubating at 95°C for 3 min. 3X gel loading buffer was added to the eluted samples, denatured at 95°C for 2 min, and loaded on an SDS-PAGE gel for western blot analysis.

RNA immunoprecipitation—quantitative-RT-PCR analysis

PUM1, PUM2 and IgG immunoprecipitations were performed O/N using PUM1 (Bethyl) and PUM2 (Abcam) antibodies with IgG antibody (CST) as negative control with cells lysed in Polysome Lysis Buffer (10 mM HEPES (pH 7.0), 100 mM KCl, 5 mM $MgCl_2$, 25 mM EDTA (pH 8), and 0.5% NP40. Prior to use, the following components were added per 50 ml of PLB buffer: one tablet of complete proteinase inhibitor (Roche), 2 mM DTT, 50 U/ml RNase OUT (Sigma) and heparin 0.2 mg/ml). The antibodies were previously conjugated with protein G streptavidin magnetic beads (Thermo Fisher). After the immunoprecipitation, the RNA was eluted from the beads with proteinase K (VWR) treatment and cDNA was prepared using High-Capacity cDNA Reverse Transcription Kit (Applied Biosystems). The qPCR analysis was performed using

Roche Fast-Start Universal SYBR green Master Mix. See Primer section for primer sequence. All experiments were performed in biological triplicates and Student's *t*-test was performed to determine statistical significance.

Localization assay (immunofluorescence)

5×10^4 cells were seeded in each well of a 24-well plate 24 h before transfection on glass coverslips and allowed to attach overnight. Cy3-labelled oligos were purchased from Sigma with the corresponding sequence (see Primers section) and transfected with RNAiMax (Thermo) using manufacturer's protocol. After 24 h, the cells were washed with 1× PBS and fixed using 4% PFA (15 min, RT) and permeabilized using ice-cold 100% MeOH (8 min, –20°C). After rehydration with 1× PBS, the cells were blocked with protein block solution (Agilent) and IFC was performed for the PUM proteins (Abcam, R&D). The coverslips were then mounted on slides using mounting media containing DAPI. The coverslips were sealed with clear polish and the slides were stored in dark, until ready to image. Olympus FV3000 confocal microscope was used for imaging these slides at 60× magnification of the objective with oil, 3× zoom using DM 488/543/633 excitation dichroics for the oligo, protein and nucleus respectively. Olympus FV31S-SW software was used for further analysis of the images.

Mature miRNA quantitative PCR

TaqMan® microRNA assays (Applied Biosystems) were used to quantify mature miRNA expression for hsa-mir-454, hsa-mir-7a and hsa-mir-10a, as previously described (87). RNU6 (Applied Biosystems) was used as endogenous control for miRNA expression studies. For miRNA expression quantification, each reverse-transcriptase (RT) reaction contained 10 ng of purified small RNAs, 1× RT buffer, dNTPs (1 mM), 5 U/μl MultiScribe reverse transcriptase, 50 nM stem–loop RT primer and 0.5 U/μl RNase inhibitor (Promega). RT reactions were incubated at 16ºC for 30 min, 42ºC for 30 min and 85ºC for 5 min. Real-time PCR reactions for miRNAs were performed in triplicate in 20 μl. The PCR reaction mix consisted of 1.33 μl of RT product, 1 μl of 20× TaqMan microRNA assay mix, and 10 μl TaqMan 2× universal PCR Master Mix. Quantitative miRNA expression data were acquired and analysed using QuantStudio™ 7 Flex Real-Time PCR System (Life Technologies).

TCGA analysis

Datasets for $\log_{10}$(RNA expression levels) were downloaded from the TCGA databases for 30 different cancer types. Pearson correlation analysis was performed using GraphPad Prism 9.0.0 software for these datasets and the correlation coefficient (*R* value) and *P* value were calculated for each dataset.

CRISPR gene editing of PRE2 of *DICER1*

Gene editing of the PRE2 in the 3′UTR of *DICER1* was performed using the Alt-R CRISPR-Cas9 System from Integrated DNA Technologies (www.idtdna.com/CRISPR-Cas9). crRNAs, tracrRNA and recombinant Cas9 (*Streptococcus pyogenes*) nuclease were ordered from IDT. gRNA targeting PRE2 was designed using the Alt-R HDR Design Tool. crRNA and tracrRNA were each dissolved with Duplex Buffer (IDT) to 200 μM and equal volumes were duplexed by incubation at 95°C for 5 min, followed by slowly cooling down to room temperature (RT). 6 μl of duplexed crRNA/tracrRNA was then combined into a Cas9 RNP complex with 8.5 μl Cas9 (from a stock solution 61 μM) in a final volume of 25 μl with phosphate-buffered saline (PBS) and incubating for 20 min at RT. ssDNA donor oligonucleotide (synthesized by IDT with PAGE purification) was resuspended in TE Buffer at a final concentration of 100 μM.

The RNP and ssDNA template was delivered into cells by electroporation using the Lonza Nucleofector 2b device and the Lonza Nucleofector Kit V. MDA-MB-231 cells were trypsinized and washed once with PBS before being resuspended at a concentration of 2.0×10^6 cells in 100 μl Nucleofector Solution (82μl and 18 μl Supplement) along with 25 μl of the RNP complex (crRNA/tracrRNA/Cas9), 5 μl of Electroporation Enhancer and ssDNA donor at a final concentration of 2 μM. After nucleofection using the X-013 program, cells were cultured in DMEM. After 48 h, cells were trypsinized and plated out at densities to allow isolation of single cell clones. These were expanded and screened for successful gene editing using a PCR mismatch assay designed to preferentially amplify mutated PRE2 from genomic DNA with PRE2-missense FOR/PRE2-missense REV primers at an annealing temperature of 62°C. Candidate clones were subsequently molecularly characterized using Next Generation Sequencing (NGS) performed at the Massachusetts General Hospital Center for Computational and Integrative Biology DNA Core. PCR with PRE2-NGS-FOR/PRE2-NGS-REV primers at an annealing temperature of 62°C was used to amplify a 210 bp region surrounding the PRE2 site which was then analyzed using Illumina-based deep sequencing. PRE sgRNA sequence, ssDNA donor sequence and primers used for NGS are found in the Primer section below.

Exome sequencing analysis

gDNA was extracted from the cell lines using Qiagen kit (#69504) following manufacturer's protocol and library was prepared. Sample quality was checked using agarose gel electrophoresis and Agilent 2100. The library was prepared using Agilent SureSelect V6. The genomic DNA was then randomly sheared into short fragments with the size of 180–280 bp. The obtained fragments were end repaired, A-tailed and further ligated with Illulmina adapters. The fragments with adapters were PCR amplified, size selected, and purified. Hybridization capture of libraries was proceeded according to the following procedures. Briefly, the prepped libraries were hybridized in the buffer with biotin-labeled probes, and magnetic beads with streptavidin were used to capture the exons of genes. Subsequently, non-hybridized fragments were washed out and probes were digested. The captured libraries were enriched by PCR amplification. The library was checked with Qubit and real-time PCR for quantification and bioanalyzer for size-distribution detec-

tion. Quantified libraries were pooled and sequenced on Illumina platforms on Novaseq 6000 PE150 system.

For each sample, there were two 'FASTQ' files. Quality and adaptor trimming was performed on each set of raw 'FASTQ' reads using TrimGalore version 0.6.0. Bowtie2 version 2.2.9 (88) was used to align the trimmed reads to the human genome (GRCh38.p12). Samtools 1.9 was used sort and merge the two different sets of reads (89,90). Samtools mpileup was used to perform a pileup of the aligned reads (89,90). Varscan version 2.4.4 was used for calling SNPs and indels (91,92). The resulting SNPs were filtered out for indels.

Mature miRNA sequencing

RNA was extracted using Qiagen miRNeasy kit. The small RNA library was prepared using NEBNext Small RNA Library Prep Kit for Illumina according to manufacturer's protocols. High throughput sequencing was performed on NovaSeq 6000 Sequencing System by Illumina using S4 flowcell. Samples were loaded on the flow cell after the concentration was calculated using the following formula: picomolar × (452/average fragment length) × 1000 = nanomolar. The picomolar value is derived from qPCR using a 6-standard curve. The average fragment length is derived from the electropherogram. For data quality control, the raw data (raw reads) of fastq format were firstly processed through in-house Perl scripts. In this step, clean data (clean reads), reads containing adapter, reads containing ploy-N, low-quality reads were counted. Errors, Q20, Q30 and GC content for the clean data were calculated. Cutadapt version 3.4 was used for trimming the TruSeq adaptor (AGATCGGAAGAGCACACGTCTGAACTCCAGTCAC). Additionally, the first base of each read was trimmed. Subsequently, reads were filtered to retain only reads of lengths 16 to 30. Bowtie2 version 2.4.4 was used to remove contaminating rRNA and tRNA reads (88,93,94). The filtered reads were aligned to the human genome GENCODE v24 and the ENCFF628BVT GTF file using STAR version 2.5.2a (95) using parameters and files as described in the ENCODE microRNA-seq Processing Pipeline (https://www.encodeproject.org/microrna/microrna-seq/) accessed 16 June 2019. The GeneCounts from the STAR alignment were input into the R version 4.0.1 and the R package DESeq2 version 1.28.1 (96) was used to perform a differential expression analysis. Significant genes were those with FDR $P < 0.20$ and $\log_2 FC > 0.3785$. The raw files are deposited on SRA (BioProject ID: PRJNA770353).

STR analysis

The gDNA was extracted from the cells using Qiagen kit (#69504) following manufacturer's protocol and STR analysis was performed at the OSUCCC Genomics core using GenePrint 10 system as per the user manual. Briefly, the PCR amplification mix was set up as described by the manufacturer and PCR was performed using GeneAmp 9700 PCR system as follows. 96°C for 1 min; 94°C for 10 s, 59°C for 1 min, 72°C for 30 s (for 30 cycles); 60°C for 10 min, 4°C hold. After this reaction, the amplified fragments were detected using Apllied Biosystems 3730 XL with POP-7 polymer. The data obtained was analyzed using Genemapper 6 and the STR table was built.

In vitro binding—liquid chromatography/mass spectrometry

RNA pull-downs assays was performed as described above. The streptavidin beads were washed with NT2 buffer (50 mM Tris–HCl (pH 7.5), 150 mM NaCl, 1 mM $MgCl_2$, 0.05% NP40), 2× at RT and with 50 mM ammonium bicarbonate buffer, 2× at room temperature. Beads were washed with 50 mM ammonium bicarbonate (25–50 ul each time depends on beads volume) three times. Each time, the supernatant were kept and pooled. After the third wash, 5 uL of DTT (5 ug/ul in 50 mM ammonium bicarbonate) is added and the sample is incubated at 65°C for 15 min. After the incubation, 5 ul of iodoacetamide (15 mg/ml in 50 mM ammonium bicarbonate) is added and the sample is kept in dark at room temperature for 30 min. 500 ng of sequencing grade-modified trypsin (Promega, Madison WI) prepared in 50 mM ammonium bicarbonate was added to the sample reaction was carried on at 37°C for overnight, additional 50 mM ammonium bicarbonate was added to make the final volume of the samples to 100 μl. The reaction is quenched the next morning by adding acetic acid for acidification. Supernatant was taken out, concentrated for LC/MSMS analysis. Capillary-liquid chromatography-nanospray tandem mass spectrometry (Capillary-LC/MS/MS) of protein identification was performed on a Thermo Scientific orbitrap Fusion mass spectrometer equipped with an EASY-Spray™ Sources operated in positive ion mode. Samples (6 μl) were separated on an easy spray nano column (Pepmap™ RSLC, C18 3μ 100 A, 75 μm ×150 mm Thermo Scientific) using a 2D RSLC HPLC system from Thermo Scientific. Each sample was injected into the μ-Precolumn Cartridge (Thermo Scientific) and desalted with 0.1% formic acid in water for 5 min. The injector port was then switched to inject and the peptides were eluted off of the trap onto the column. Mobile phase A was 0.1% Formic Acid in water and acetonitrile (with 0.1% formic acid) was used as mobile phase B. Flow rate was set at 300 nl/min. Typically, for in gel digestion samples, mobile phase B was increased from 2% to 5% in 5 min and then increased from 5 to 16% in 100min and again from 16 to 25% in 20 min. Mobile phase B was increased again to 85% in 1 min and then kept at 85% for another 4 min before being brought back quickly to 2% in 1 min. The column was equilibrated at 2% of mobile phase B (or 98% A) for 14 min before the next sample injection. MS/MS data was acquired with a spray voltage of 1.6 KV and a capillary temperature of 305°C is used. The scan sequence of the mass spectrometer was based on the preview mode data dependent TopSpeed™ method: the analysis was programmed for a full scan recorded between m/z 375–1500 and a MS/MS scan to generate product ion spectra to determine amino acid sequence in consecutive scans starting from the most abundant peaks in the spectrum in the next 3 s. To achieve high mass accuracy MS determination, the full scan was performed at FT mode and the resolution was set at 120 000 with internal mass calibration. The AGC Target ion number for FT full scan was set at 4×10^5 ions,

maximum ion injection time was set at 50 ms and micro scan number was set at 1. MSn was performed using HCD in ion trap mode to ensure the highest signal intensity of MSn spectra. The HCD collision energy was set at 32%. The AGC Target ion number for ion trap MSn scan was set at 3.0E4 ions, maximum ion injection time was set at 35 ms and micro scan number was set at 1. Dynamic exclusion is enabled with a repeat count of 1 within 60 s and a low mass width and high mass width of 10 ppm. Sequence information from the MS/MS data was processed by converting the .raw files into a merged file (.mgf) using MSConvert (ProteoWizard). Isotope distributions for the precursor ions of the MS/MS spectra were deconvoluted to obtain the charge states and monoisotopic m/z values of the precursor ions during the data conversion. The resulting mgf files were searched using Mascot Daemon by Matrix Science version 2.5.1 (Boston, MA) and the database searched against the most recent Uniprot databases (97). The mass accuracy of the precursor ions were set to 5ppm, accidental pick of 1 ^{13}C peaks was also included into the search. The fragment mass tolerance was set to 0.5 Da. Carbamidomethylation (Cys) is used as a fixed modification and considered variable modifications were oxidation (Met) and deamidation (N and Q). Four missed cleavages for the enzyme were permitted. A decoy database was also searched to determine the false discovery rate (FDR) and peptides were filtered according at 1% FDR. Proteins identified with at least two unique peptides were considered as reliable identification. Any modified peptides are manually checked for validation. Label free quantitation was performed using the spectral count approach, in which the relative protein quantitation is measured by comparing the number of MS/MS spectra identified from the same protein in each of the multiple LC/MSMS datasets. Scaffold was used for data analysis. Student-t test was performed by scaffold to evaluate if the fold change for certain proteins is significant ($P < 0.05$). The raw files are deposited on MassIVE proteomics repository (https://doi.org/doi:10.25345/C5F47GZ2W).

Metabolic labelling for RNA stability

RNA stability analysis was performed as mentioned in Russo *et al.* (98). Briefly, cells were treated with 4sU to a final concentration of 500 μM and incubated for 2 h + 5 min, covered with aluminum foil, in a 37°C incubator with 5% CO_2. At the end of this incubation, cells were washed with 1× PBS and total RNA was extracted using Trizol (Thermo Fisher). RNA quality was assessed using Agilent RNA tape station analysis. 50 μg of the total RNA was biotinylated in a reaction mixture (50 μg 4sU labelled RNA, 15 μl 10× biotinylation buffer (100 mM HEPES, 10 mM EDTA), 10 μl 1 mg/ml HPDP-biotin) with 30 min incubation at RT in the dark. RNA was then precipitated and concentration was measured. The samples were then adjusted to have the same concentration and a 50 μl aliquot of 'total RNA' was reserved for all samples. A second 50 μl aliquot was mixed with 100 μl of magnetic streptavidin beads and incubated at RT in the dark with gentle agitation for 15 min. The beads were then washed 2X using washing buffer (100 mM Tris, 10 mM EDTA, 1 M NaCl, 0.1% Tween-20). RNA was eluted from the beads using 100 μl of 100 mM DTT as the elution buffer and with 5 min incubation at RT. The eluate was removed and the elution step was repeated with another 100 μl of 100 mM DTT. 150 μl of 100 mM DTT was added to the 'total RNA' sample and the RNA from all the samples were ethanol precipitated. The RNA eluted from the beads are called 'nascent RNA'. The RNA was used for reverse transcription with the RT-PCR kit (Applied Biosystems) with 3:1 random primers:oligo dT. Target-specific primers were used for further quantitative real-time PCR analysis. Half-life of the mRNA transcript was calculated with the formula:

$$t_{1/2} = -t_L * \ln(2) / \ln(1 - R)$$

where t_L = labeling time (minus 5 min incorporating time), R = abundance in nascent RNA fraction/abundance in total RNA fraction.

Actinomycin-D treatment for RNA stability

MDA-MB-231 cells were treated for indicated times (4 h, 8 h) with 2 ug/ml of Actinomycin-D. 250 ng of total RNA was used for q-RT-PCR to measure the level of DICER1 mRNA relative to b-Act mRNA using primers mentioned below. Comparitive Ct method was used to calculate the relative mRNA levels and GraphPad Prism was used for further analysis.

PUM1 and AUF1 protein expression and purification

AUF1 (Plasmid #135939) was obtained from Addgene and expressed and purified as previously reported (99). Rosetta™ Competent Cells—(Novagen) were transformed with pET28a His6-AUF1 (p37) and grown at 37°C. A single colony was inoculated in small culture containing kanamycin overnight at 37°C with shaking. Next day, the bulk culture of 400 ml containing kanamycin was diluted with small culture and grown at 37°C with shaking to optical density $(OD)_{600}$ = 0.5 at which point isopropyl-β-D-thiogalactoside (0.20 mM final concentration; Sigma aldrich) was added to induce expression. The temperature was then reduced to 16°C, and cultures were grown overnight with shaking. Cells were harvested by centrifugation (6000 g, 20 min, 4°C), and lysed in lysis buffer [20 mM Tris pH 7.5, 500 mM KCl, 2 mM $MgCl_2$, 10 mM imidazole (Thermo Fisher Scientific), 5% glycerol, 5 mM β-mercaptoethanol (βME), and 0.5 mM phenylmethylsulfonyl fluoride (Enzo Life Sciences, Farmingdale, NY, USA). Debris was cleared using centrifugation (20 000 g, 30 min, 4°C). Streptomycin sulfate (1% wt/vol) was added dropwise over 20 min with gentle stirring, and precipitated material was cleared by centrifugation (20 000 g, 30 min, 4°C). The lysate then was incubated with nickel resin (Qiagen) for 1 h with gentle agitation. The resin was washed progressively with wash buffers (20 mM Tris pH 7.5; 150 mM KCl; 2 mM $MgCl_2$; 50, 100, 200 mM imidazole; and 5 mM βME). Protein was eluted with elution buffer (20 mM Tris pH 7.5, 150 mM KCl, 2 mM $MgCl_2$, 300 mM imidazole). PUM1 expression and purification was done as previously reported. Briefly, Rosetta cells were transformed with PUM1_PDEST527 and grown as described above. The protein was induced with isopropyl-β-D-thiogalactoside

(0.25 mM final concentration; Sigma aldrich) at 16°C for overnight. Cells were pelleted, lysed using the lysis buffer (20 mM Tris pH 7.5, 500 mM KCl, 2 mM $MgCl_2$, 5% glycerol, 5 mM β-mercaptoethanol (βME), and 0.5 mM phenylmethylsulfonyl fluoride (Enzo Life Sciences, Farmingdale, NY, USA)) for 30 min in the presence of protease inhibitor cocktail (Roche), sonicated and clarified by centrifuging at > 8,000 rpm, passed through a .45 μM filter (GE) and purified using nickel resin.

RNA EMSA with AUF and PUM1

All EMSA experiments were performed as previously reported with the following adaptions. DNA oligonucleotides were obtained from Sigma Aldrich and *in vitro transcribed* using the T7 RNA polymerase enzyme (Sigma Aldrich) as described by manufacturer. RNA oligonucleotides were radiolabeled at the 5′ end by using [γ-32P]ATP (PerkinElmer Life Sciences, Wellesley, MA) and T4 polynucleotide kinase (New England BioLabs, Ipswich, MA) by following manufacturer directions. Binding reactions included ≈50 pM radiolabeled RNA and varying concentrations of protein (AUF1 and PUM1) incubated in binding buffer (10 mM HEPES, pH 7.4/50 mM KCl/1 mM EDTA/0.01% (vol/vol) Tween-20/0.1 mg/ml BSA/1 mM DTT). Binding reactions were incubated 30–45 min at RT and immediately analyzed by electrophoresis on 8% non-denaturing polyacrylamide gel run in 0.5× TBE at 50–70 V at 4°C. Gels were dried and exposed to storage phosphor screens (GE Healthcare, Piscataway, NJ) for 5–10 days, scanned with a Typhoon 8600 Imager (GE Healthcare), and analyzed with Image Quant 5.2 software (GE Healthcare).

ChIP-qPCR analysis

Chromatin immunoprecipitation (ChIP) was performed as described (100), with some modifications. The cells per condition were cross-linked with 1% formaldehyde added to the media for 15 min at RT. After quenching with 0.125 M glycine, fixed cells were washed twice with PBS containing 1 μM PMSF and protease inhibitors, pelleted and lysed in lysis buffer (1%SDS, 10 mM EDTA, 50 mM Tris–HCl pH 8.1) at 2×10^7 cells/ml. Sonication was performed with a Covaris system (shearing time 20 min, 20% duty cycle, intensity 6, 200 cycles per burst and 30 s per cycle). 1×10^7 cells equivalent to 40–50 μg of chromatin were used per immunoprecipitation reaction with 10 μg of Phospho-RNA polymerase 2 CTD repeat YSPTSPS (Ser2) Polyclonal Antibody (Thermo, BS-6581R). ChIP-qPCR on immunoprecipitated chromatin was performed using the SYBR Green PCR Master Mix and reactions were performed in triplicate. The corresponding primers are listed in primer section as ChIP primers. The relative amount of each amplified fragment was estimated with respect to the amplification obtained from input DNA and normalized against a negative group-IgG using the ΔΔCt method.

Statistical analysis

All experiment were performed in biological triplicates and the individual values of these replicates are plotted. The error bars represent standard deviation of these replicates. Statistical analysis was performed by two-tailed unpaired student's t-test on GraphPad Prism 9.0.0 software. $*P < 0.05$, $**P < 0.01$, $***P < 0.001$, $****P < 0.0001$.

Primers

Target	Forward	Reverse
E2F4	TCACAGAGGACGTGCAGAAC	AGGGTATCTCCAGCAAAGCA
DICER1	CATGACCCCTGCTTCCTCAC	GCTCCAGTATTAGTGTTCGCA
DGCR8	CAAGCAGGAGACATCGGACAAG	CACAATGGACATCTTGGGCTTC
DROSHA	TAGGCTGTGGGAAAGGACCAAG	GTTCGATGAACCGCTTCTGATG
pre-miR-301b	CAGGTGCTCTGACGAGGTTG	TGGTCCCAGATGCTTTGACA
pre-miR-128	TGGTCCCAGATGCTTTGACA	AAGCAGCTGAAGAAGAGACCG
pre-miR-21	GTCGGGTAGCTTATCAGAC	GACAGCCCATCGACTG
3′UTR DICER	TAATACGACTCACTATAGGGAGACGCCAATAGCAATAT	AGAGAACAGACGATAACTTTATTGG
3′UTR VEGFA	TAATACGACTCACTATAGGGTCCCGGCGAAGAGAAGAGAC	GGGAGGGCAGAGCTGAGTGTTA
3′UTR MRAS	TAATACGACTCACTATAGGGACATACAAGCTGGTGGTG	CACATTGCAGTTTGTGGG
DICER1 polyA site 4071	GGACATCAACCACAGACAA	CAAGCAGAAGACGGCATACGAGATTTTTTTTTTTTTTTTTTTTT
DICER1 polyA site 4245	TTCATTCATACAGTAATCATGCTGC	CAAGCAGAAGACGGCATACGAGATTTTTTTTTTTTTTTTTTTT
β-actin	TCACCCACACTGTGCCCATCTACG	CAGCGGAACCGCTCATTGCCAATG
PUM1-FL-EcoRVFwd	GATAGATATCATGAGCGTTGCATGTGTCTTG	
PUM1-HD-NotIRev		CTATGCGGCCGCGATGATACCATTAGGGGGGC
PUM2-HD-EcoRVFwd	GATAGATATCATGCCTCTGCCAAGCCAAAC	
PUM2-HD-NotIRev		CTATGCGGCCGCCAGCATTCCATTTGGTGGTC
PRE2 sgRNA - Alt-R crRNA	/AltR1/rUrUrUrUrCrUrGrCrUrGrUrArArArUrArGrUrGrArGrUrUrUrUrArGrArGrCrUrArUrGrCrU/AltR2/	
ssDNA donor:	AAT ATG CAT TAG TTT TAC TT G ATT TTA GTA ATT TTC CTT C ACTAT TTG GAG CAG AAA A GC CAG AAA TTT ACT TCC T GT TCA CCT TTG CAT	
Mismatch primers	GTAAATTTCTGGCTTTTCTGCTCC	AAAGGTAATTGTGATCCATAAGGTG
Primers for NGS	TTTGGACATCAACCACAGACA,	AGCTGCAGCATGTGATGGTA
Cy3-DICER1-WT	UCUGCUGUUAAAUAGUGAAGG	
Cy3-DICER1-MUT	UCUGCUCCUAAAUAGUGAAGG	
DICER1-WT-Gibson	AATTCTAGGCGATCGCTCGAGTTGGAGACGCCAATAGC	AAACGAATTCCCGGGCTCGACCTTCACTATTTACAGCAGA
DICER1-pMut-Gibson	AATTCTAGGCGATCGCTCGAGTTGGAGACGCCAATAGC	AAACGAATTCCCGGGCTCGACCTTCACCATTTACAGCAGA
DICER1-T7-PRE1	TAATACGACTCACTATAGGGCCCCACTTTAGAGCCCTGTG	AACTGCGCTCGATCTGGATT
DICER1 ChIP	CAGGAGCCCTTTTCAAGCTGA	GGGATGTGTTGGGGAGTGAG

RESULTS

To determine the putative post-transcriptional mechanisms regulating DICER1 levels, we cross-referenced RBP motifs identified by MEME with published CLIP datasets. From this analysis, we found two putative PUM Regulatory Elements (PRE), UGUAHAUA, within the DICER1 3′UTR (Figure 1A, Supplementary Figure S1A). The dis-

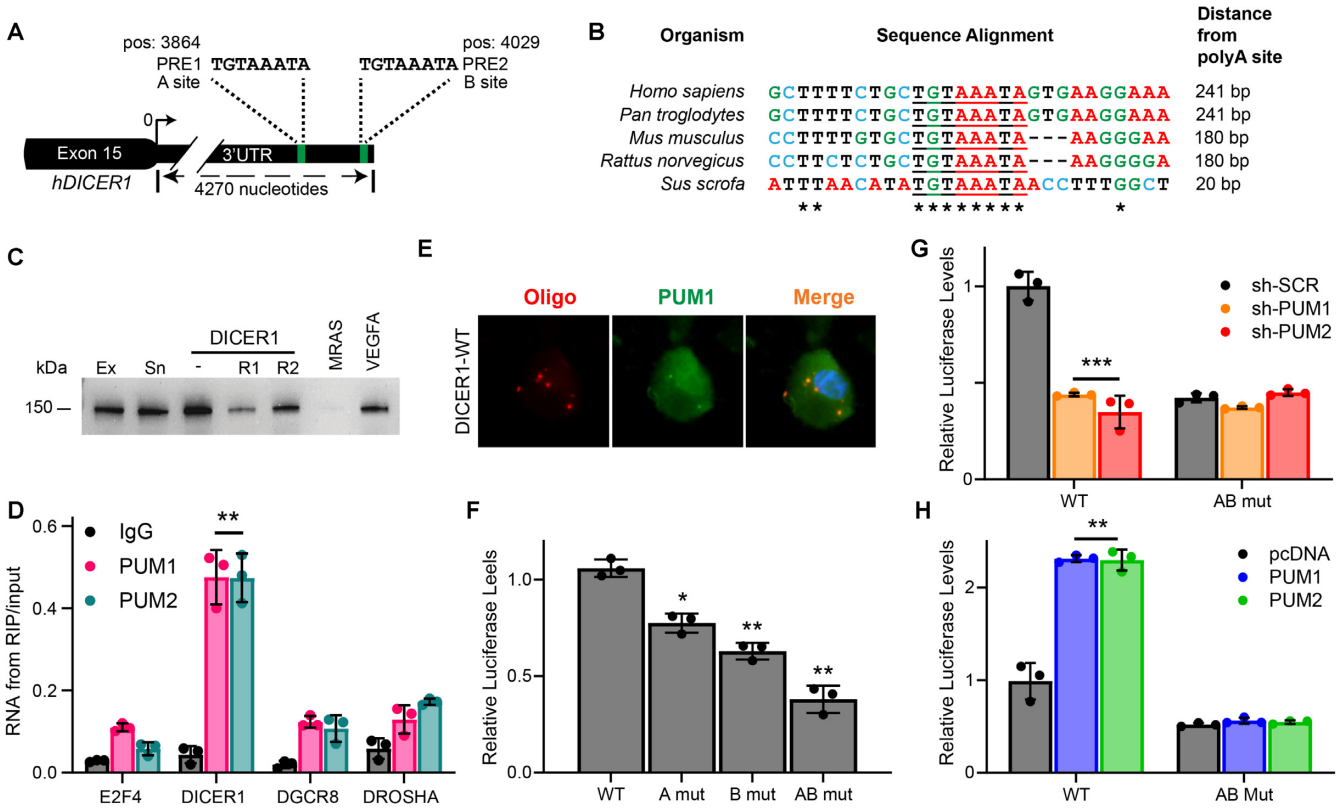

Figure 1. The DICER 1 3′UTR contains a function PUM Regulatory Element. (**A**) Schematic of the human *DICER1* 3′UTR region showing the position of the two putative PREs (TGTAAATA). (**B**) Sequence conservation of the distal PRE sequence in *DICER1*-3′UTR across mammalian species and its respective distance from the polyA site. The putative PRE site is underlined in the sequence alignment and highly conserved nucleotides are marked by a * symbol. (**C**) PUM1 *in vitro* RNA binding assays of the DICER1 WT sequences. Ex: Extract Input alone, Sn:Supernatant flow through alone, DICER1 RNA plus: -: TAP-Tagged PUM1 expressing extract, R1: – + PRE containing non-biotinylated oligo, R2: – + non-PRE containing non-biotinylated oligo, MRAS RNA (non-PUM substrate) and VEGFA (PUM substrate). (**D**) Relative E2F4 (negative control), DICER1, DROSHA and DCGR8 RNA bound to IgG, PUM1 and PUM2 from RIP-qPCR analysis from MDA-MB-231 cells. n = 3 biological replicates. Error bars represent standard deviations from these replicates. $^{**}P < 0.01$. (**E**) Representative confocal microscopy images of Cy3-labelled WT RNA (red), PUM1 (green) and DAPI (blue) from RPE1 cells. Inset image scale bar = 2 μm. (**F**) Relative Luciferase levels from MDA-MB-231 cells transfected with a Luciferase reporter gene followed by a WT DICER1 3′UTR region (WT), PRE1 (A mut), PRE2 (B mut) or PRE1 and 2 (AB mut) disrupting mutations. (**G**) Relative Luciferase levels from MDA-MB-231 cells infected with shRNAs targeting a Scrambled control sequence (sh-SCR), PUM1 (sh-PUM1) or PUM2 (sh-PUM2) and transfected with a Luciferase gene followed by a WT DICER1 3′UTR region (WT), or PRE1 and 2 (AB mut) disrupting mutations. (**H**) Relative Luciferase levels from MDA-MB-231 cells transfected with a control pcDNA plasmid, HA-PUM1 or HA-PUM2 and transfected a Luciferase gene followed by a WT DICER1 3′UTR region (WT), or PRE1 and 2 (AB mut) disrupting mutations. *n* = 3 biological replicates. Error bars represent standard deviations from these replicates. $^{*}P < 0.05$, $^{**}P < 0.01$, $^{***}P < 0.001$, $^{****}P < 0.0001$.

tal PRE motif is located close to the poly-adenylation signal, >250bp, in agreement with published data showing functional PREs are enriched at distal regions of 3′UTRs of their substrates (101). This motif is highly conserved in mammals, in contrast to both 5′ and 3′ flanking regions (Figure 1B). To test whether the human PUM1 protein could interact with the *DICER1* 3′UTR, we expressed TAP-tagged PUM1 in HEK 293T cells. Protein extracts from these cells were then used for *in vitro* RNA binding assays. We found that PUM1 binds strongly to the *DICER1* 3′UTR (WT) and established PUM1 substrate, VEGFA (59) *in vitro* (Figure 1C). This interaction is specific, as the addition of the non-labeled PRE oligo (R1), can compete with the DICER1 3′UTR for PUM1 binding (Figure 1C). In contrast, the addition of a non-PRE containing oligo (R2), did not alter the levels of PUM1 interaction. This data shows that PUM1 can interact with the *DICER1* 3′UTR *in vitro*. We next analyzed published PUM-CLIP (102) and RIP-chip datasets (59), and found that the DICER1 transcript is bound by the PUM proteins. To determine whether *DICER1* is the sole miRNA processing gene regulated by the PUM proteins, we conducted PUM1, PUM2 and IgG (control) RNA-binding protein immunoprecipitations (RIPs) from 3 independent cell lines from diverse tissue lineages: MDA-MB-231 (breast), RPE1 (retinal), and DLD1 (colorectal). RIP experiments followed by relative RT-PCR analysis showed that PUM1 and PUM2 are significantly associated with the *DICER1* mRNA (Figure 1D). In contrast, DROSHA and DCGR8 that do not have PRE motifs, are not bound by PUM1 or PUM2, and display similar RIP-RT-PCR levels to the non-PUM substrate, E2F4 (77) (Figure 1D, Supplementary Figure S1B, C). We then tested whether endogenous PUM1 co-localized with Cy3-labeled DICER1 3′UTR RNA probes and found both PUM1 and the *DICER1* RNA in cytoplasmic foci (Figure 1E). The data from both *in vitro* RNA-RBP pull-

down and RIP-RT-PCR assays shows that the PUM proteins bind to the *DICER1* RNA *in vitro* and *in vivo*.

The PREs within the *DICER1* 3′UTR are functional and important for regulating DICER1 protein levels

To define the effect of PUM regulation on *DICER1*, we cloned the WT *DICER1* 3′UTR downstream of a Luciferase (LUC) reporter gene and utilized site-directed mutagenesis to disrupt the putative PREs (UGUAAAUA > UCCAAAUA). This strategy generated multiple reporter plasmids that have PRE-disabling mutations in the proximal PRE (A mut), distal PRE (B mut) or both PREs (AB mut). These plasmids were then transfected into MDA-MB-231, RPE1 and DLD1 cells and the relative LUC levels were measured. Disruption of a single PRE site significantly reduced LUC levels, while the mutation of both PREs showed an additive reduction compared to WT (Figure 1F, Supplementary Figure S1D, E). To test whether these effects were due to disrupted PUM binding, we assayed how the depletion of PUM1 or PUM2 altered LUC levels from WT or the AB MUT plasmid. For this, we utilized two independent short hairpin RNAs (shRNAs) to silence PUM1, PUM2, or a control Scrambled (SCR) sequence (Supplementary Figure S1F). PUM-depleted MDA-MB-231 cells were transfected with either WT or AB MUT plasmids, and the relative LUC measured. These experiments showed that PUM1 or PUM2 depleted cells have significantly lower levels of WT LUC relative to SCR control (Figure 1G, Supplementary Figure S1G, H). In contrast, LUC levels were unchanged in cells containing the AB MUT (Figure 1G, Supplementary Figure S1G, H), indicating that PUM exerts regulation via PRE motifs. We then tested how elevated PUM levels affected WT and AB LUC production. HA-tagged PUM1, HA-PUM2 or pcDNA empty vector control were transfected to WT and AB LUC expressing cells. We found that the over-expression of PUM1 or PUM2, increased WT LUC levels (Figure 1H, Supplementary Figure S1I, J), however AB LUC levels were unchanged (Figure 1H, Supplementary Figure S1I, J). These results demonstrate that PUM protein levels and PRE function are important for DICER1 3′UTR regulation. Interestingly, our data shows that the PUM proteins positively regulate DICER1 levels, this is in contrast to the majority of PUM targets, where PUM acts as a negative regulator (57).

PUM and *DICER1* levels correlate across cancer

To determine how PUM affects endogenous *DICER1* mRNA and protein levels, we overexpressed PUM1 in MDA-MB-231 cells and measure DICER1 protein levels using western blots. We found that elevated PUM1 protein levels, resulted in increased DICER1 protein levels, relative to pcDNA control (Figure 2A). In agreement, CRISPR-Cas9 generated *PUM1*$^{-/-}$, *PUM2*$^{-/-}$ or *PUM1*$^{-/-}$ *PUM2*$^{-/-}$HCT116 cells (103) also have diminished DICER1 protein levels, relative to WT controls (Figure 2B). As DICER1 functions to process pre-miRNAs into mature miRNAs, we assayed how changes in PUM levels affected pre-miRNA processing in MDA-MB-231 cells. We found significantly elevated pre-miRNA levels of pre-miR-10a, pre-miR-454 and pre-miR-129 (104) in PUM1 and PUM2 knock-out cells, relative to control (Figure 2C). In agreement, the mature miRNA levels of each candidate miRNAs were reduced (Supplementary Figure S2A). Conversely, PUM1 over-expression increased the levels of mature miRNAs, miR-10a, miR-454 and miR-129, and reduced pre-miR levels, relative to the pcDNA control (Figure 2D, Supplementary Figure S2B). These results suggest that PUM is a direct regulator of DICER1 levels in different cell types and is required to sustain DICER1 protein levels and miRNA processing.

To measure whether PUM was a regulator of DICER1 RNA, we depleted or over-expressed PUM1 and PUM2 in MDA-MB-231 cells and measured DICER1 levels using RT-PCR. shRNA-mediated silencing of either PUM protein significantly reduced DICER1 RNA levels (Figure 2E). In contrast, PUM over-expression increased the levels of the DICER1 RNA (Figure 2F). To evaluate whether this tight correlation between PUM and DICER1 levels was also found in tumor datasets, we analyzed the correlation between *PUM1, PUM2* and *DICER1* in each tumor type within the TCGA dataset (Supplementary Table S1). In this analysis, the constitutively expressed house-keeping gene, *Tubulin (TUB)*, was used as a negative control. We found that *PUM1* (blue) and *PUM2* (green) show strong and statistically significant linear correlations (R correlations) with *DICER1* levels (Figure 2G, H). In contrast, *TUB* and *DICER1* levels do not correlate, and in no tumor type does *TUB* have a stronger R-correlation with *DICER1* than *PUM1* or *PUM2* (Figure 2G, H). We next measured the correlation of *PUM1, PUM2, TUB* and *DICER1* levels across the entire TCGA dataset. We found that *PUM1* ($R = 0.2429$) (Figure 2I) and *PUM2* ($R = 0.2809$) (Figure 2J) correlated significantly (PUM1: $P < 0.0001$; PUM2: $P < 0.0001$) with *DICER1* levels relative to *TUB* ($R = 0.0184$, $P = 0.0781$) (Figure 2K). This data suggests that the correlated levels between *PUM1, PUM2* and *DICER1* are due to a regulatory mechanism that is conserved across cancer types.

DICER1 syndrome allele, *rs1252940486*, disrupts PUM binding to the DICER1 3′UTR

To determine the fidelity of this regulation in the human population, we analyzed publicly available Nucleotide Polymorphism (SNP) datasets. This identified a previously uncharacterized SNP, *rs1252940486*. This SNP changes the final base within the PRE motif (A > G), producing a non-canonical PRE sequence (Figure 3A, Supplementary Figure S3A) and was identified in a patient with a DICER1 syndrome. DICER1 syndrome is cancer pre-deposition disorder caused by the loss of DICER1 function. This suggested that PUM regulation of DICER1 may be important for normal DICER1 levels. To determine how the DICER1 syndrome SNP, *rs1252940486*, here after referred to as A > G, altered PUM interaction and co-localization, we conducted *in vitro* PUM1 binding assays and Immunofluorescence (IF). The A > G mutation significantly diminishes PUM1 binding, relative to the WT DICER1 3′UTR sequence (Figure 3B). In addition, PUM1 and PUM2 do not co-localize with Cy3-labeled DICER1 A > G RNA (Fig-

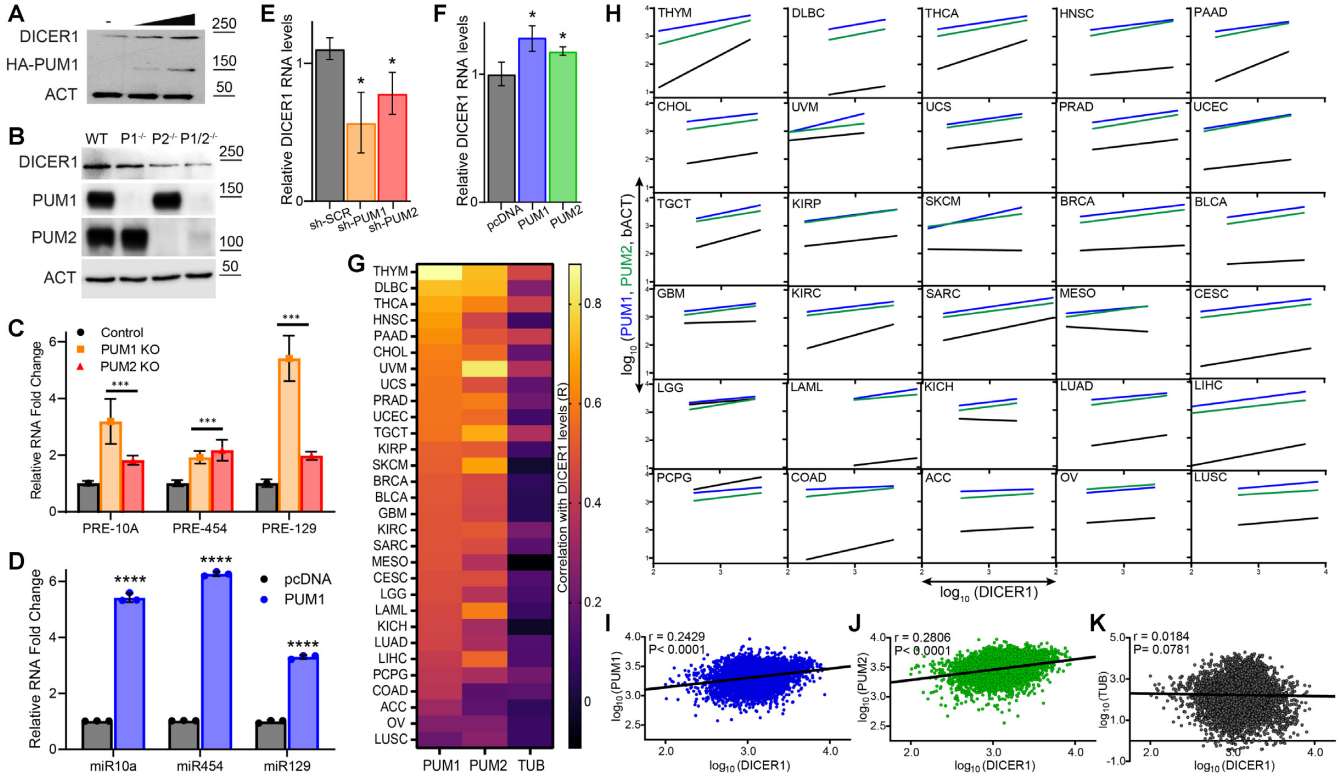

Figure 2. DICER1 and PUM levels correlate. (**A**) Western blots of DICER1, HA and ACT from MDA-MB-231 cells transfected with a control pcDNA plasmid or increasing concentrations of HA-PUM1. (**B**) Western blots of DICER1, PUM1, PUM2 and ACT from CRISPR-Cas9 edited *WT*, *PUM1*$^{-/-}$, *PUM2*$^{-/-}$ and *PUM1/2*$^{-/-}$ HCT116 cells. (**C**) Relative pre-miRNA levels of pre-miR-301b, pre-miR-128 and pre-miR-21 (non-DICER1 substrate) from MDA-MB-231 cells infected with shRNAs targeting a scrambled control sequence (sh-SCR), PUM1 (sh-PUM1) or PUM2 (sh-PUM2). (**D**) Relative mature miRNA levels of miR-10a, miR-454 and miR-129 from MDA-MB231 cells transfected with pCDNA (control) and HA-PUM1 plasmids. (**E**) Relative DICER1 RNA levels from MDA-MB-231 cells infected with shRNAs targeting a scrambled control sequence (sh-SCR), PUM1 (sh-PUM1) or PUM2 (sh-PUM2). (**F**) Relative DICER1 RNA levels from MDA-MB231 cells transfected with pCDNA (control), HA-PUM1 and HA-PUM2 plasmids. (**G**) Heat map of R values from linear regression analysis between DICER1 and PUM1, PUM2 and TUB (control) RNA levels in 30 TCGA tumor datasets. (**H**) Linear regression between DICER1 and PUM1 (blue), PUM2 (green) and TUB (black) (control) RNA levels across 30 TCGA tumor datasets. List of abbreviation along with R values and p values are found in Supplementary Table S1. (**I**) Scatter plots, linear regression and correlation analysis of DICER1 and PUM1 levels from each tumor in the pan-cancer TCGA dataset. (**J**) Scatter plots, linear regression and correlation analysis of DICER1 and PUM2 levels from each tumor in the pan-cancer TCGA dataset. (**K**) Scatter plots, linear regression and correlation analysis of DICER1 and TUB levels from each tumor in the pan-cancer TCGA dataset. $n = 3$ biological replicates. Error bars represent standard deviations from these replicates. $^{*}P < 0.05$, $^{**}P < 0.01$, $^{***}P < 0.001$, $^{****}P < 0.0001$.

ure 3C). To evaluate whether the A > G mutation changed the regulation of the *DICER1* 3′UTR, we cloned the wild-type (WT) and A > G region (3975–4076 bp) downstream of a LUC reporter gene and transfected them into HCT116 cells. The A > G mutation reduced LUC production (Figure 3D), relative to the WT sequence. Our data shows that the *rs1252940486* mutation disrupts PUM regulation of DICER1.

Disrupting endogenous PUM regulation of DICER1 alters miRNA production

No model or tissue of the DICER1 syndrome patient with the *rs1252940486* mutation exist. This prevents us from testing how *rs1252940486* contributes to DICER1 syndrome. However disrupting this PRE in a tumor fueled by high DICER1 levels will enable us to test the importance of this regulation to tumorigenesis. For this, we selected MDA-MB-231 triple-negative breast cancer (TNBC) cells as: (i) they have very high *PUM1:DICER1* ($R = 0.4662$, $P < 0.0001$) and *PUM2:DICER1* ($R = 0.4089$, $P < 0.0001$) correlations, (ii) DICER1 levels are prognostic for TNBC patients (40) and (iii) alterations in DICER1 levels change the tumorigenic properties of these cells. Using CRISPR-Cas9 engineering, we generated targeted knock-in (KI) clonal cell lines containing PRE-disruptions or PRE-disabling mutations in the distal PRE (TGTAAATA > TCCAAATA). High sgRNA off-target spectrums prevented the production of A > G mutations. We generated three independent biological clonal cell lines (C1, C2 and C3) from single cells, with PRE mutations (Figure 3E). Whole genome sequencing of each cell line confirmed only on-target editing of the PRE2 site in the *DICER1* gene and no evidence of changes in any of the predicted off-target sites (Supplementary Figure S3B). Short Tandem Repeat (STR) analysis was used to confirm that each cell line was MDA-MB-231 (Supplementary Figure S3C). To measure DICER1 protein levels in these cells, we used western blots and found significantly lower DICER1 protein levels in C1-C3 cells, compared to WT control cells (Figure 3F). Poly-A site usage

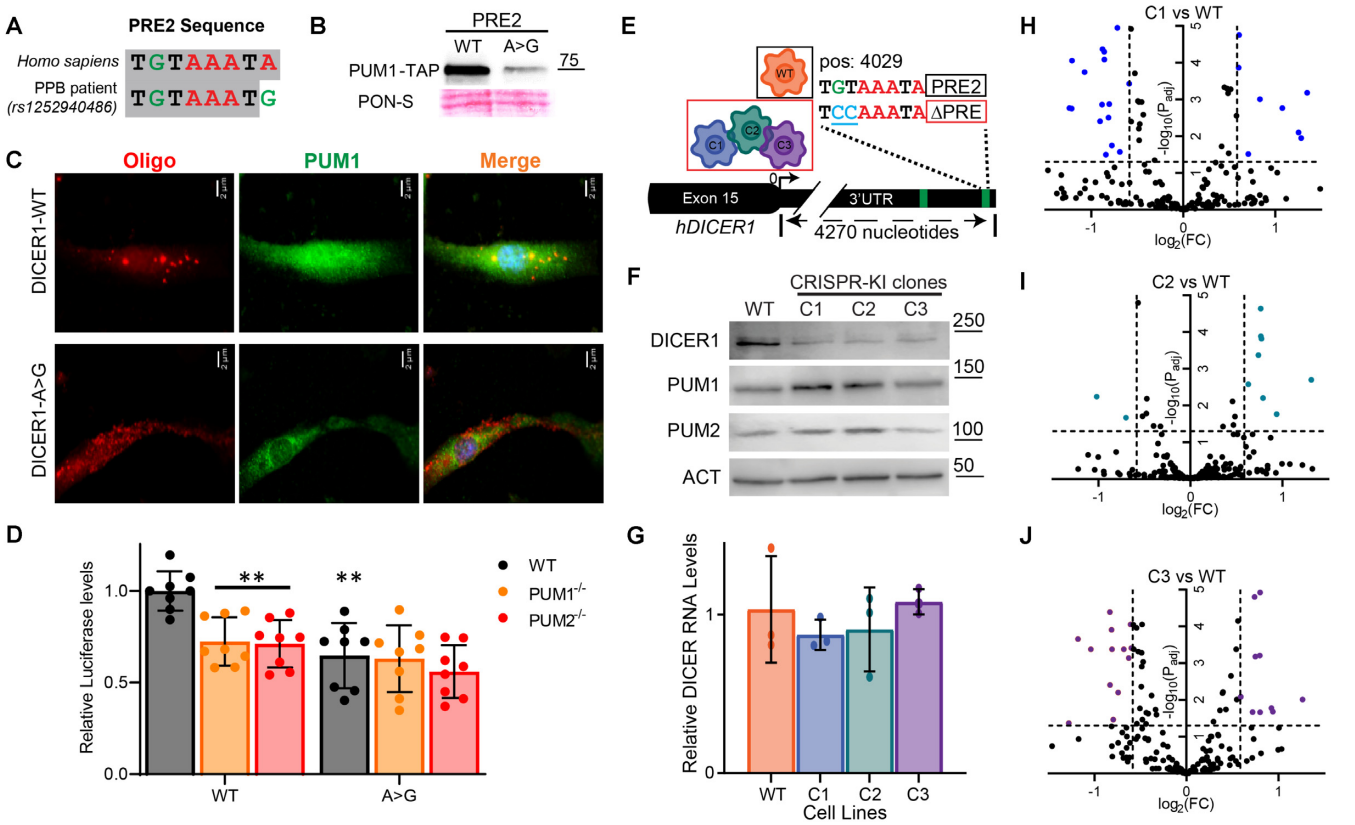

Figure 3. Disruption of the DICER1 distal PRE, alters DICER1 protein levels and miRNA production. (**A**) The PRE sequence and *rs1252940486* (A > G) patient mutation. (**B**) RNA pull-down assays of the DICER1 3′UTR PRE2 region comparing WT and the A > G sequence. (**C**) Representative confocal microscopy images of Cy3-labelled DICER1 WT (DICER1-WT) or A > G (DICER1-A > G) RNA (red), PUM1 and PUM2 (green) and DAPI (blue) from RPE1 cells. (**D**) Relative Luciferase levels from WT, PUM1$^{-/-}$ and PUM2$^{-/-}$ HCT116 cells transfected with a Luciferase reporter gene followed by a WT DICER1 3′UTR region (WT) or A > G sequence. $n = 3$ biological replicates. Error bars represent standard deviations from these replicates. $^{**}P < 0.01$. (**E**) Schematic of CRISPR-Cas9 mediated alteration of PRE2 within the DICER1 3′UTR. (**F**) Western blots of DICER1, PUM1, PUM2 and ACT from WT, and C1-C3 MDA-MB-231 cells. (**G**) Relative mRNA levels of DICER1 from WT, and C1-C3 MDA-MB-231 cells. (**H**) Volcano plots of $\log_2$ fold mature miRNA changes in C1 CRISPR-Cas9 edited MDA-MB-231 cells relative to WT. Blue dots highlight significantly altered miRNAs. (**I**) Volcano plots of $\log_2$ fold mature miRNA changes in C2 CRISPR-Cas9 edited MDA-MB-231 cells relative to WT. Green dots highlight significantly altered miRNAs. (**J**) Volcano plots of $\log_2$ fold mature miRNA changes in C3 CRISPR-Cas9 edited MDA-MB-231 cells relative to WT. Orange dots highlight significantly altered miRNAs.

(Supplementary Figure S3D) and total DICER1 RNA levels (Figure 3G, Supplementary Figure S4A/B) was not altered. Using miRNA sequencing, we found widespread and conserved changes in miRNA levels in C1–C3 cells (Figure 3H-J, Supplementary Table S2). In agreement with data from other DICER1 loss of function studies in human cell lines (105), we find that miRNA levels are both up- and down-regulated. These results demonstrate that the disruption of PRE2 with DICER1, significantly alters DICER1 proteins levels and miRNA processing.

PUM protects *DICER1* mRNA from AUF1-mediated degradation

Human cells have a large network of post-transcriptional regulators including RBPs and miRNAs that actively compete for RNA motifs and structures. Mutations that disrupt one interaction, such as *rs1252940486*, found in a DICER1 syndrome patient, may provide binding opportunities for additional RBPs, due to altered secondary structure or RNA-binding motifs. To assess this, we used RNAfold (106) to determine how PRE2 mutations affect RNA folding of the DICER1-3′UTR. We found that the RNA secondary structure of the *rs1252940486 DICER1* 3′UTR remained unchanged compared to WT (Supplementary Figures S5A, B). To define how the *rs1252940486* mutation altered spectrum of RBPs bound to the *DICER1* RNA, we utilized biotinylated WT or A > G RNA as baits to capture endogenous RBPs for mass spectrometry analysis. We found that the AUF1, LARP4 and STAU2 RBPs were all enriched on the A > G RNA relative to WT control (Figure 4A, Supplementary Table S3). We next tested how the independent depletion of each candidate RBPs altered DICER1 protein levels, relative to SCR controls. Depletion of AUF1, but not LARP4 and STAU2, increased DICER1 RNA (Figure 4B, Supplementary Figure S5C, D) and protein levels (Supplementary Figure S5E)—in WT, C1 and C2 cell lines. We therefore focused on the relationship between PUM1 and AUF1 in regulating DICER1. We conducted RNA *in vitro* binding assays from cell extract that contained TAP-

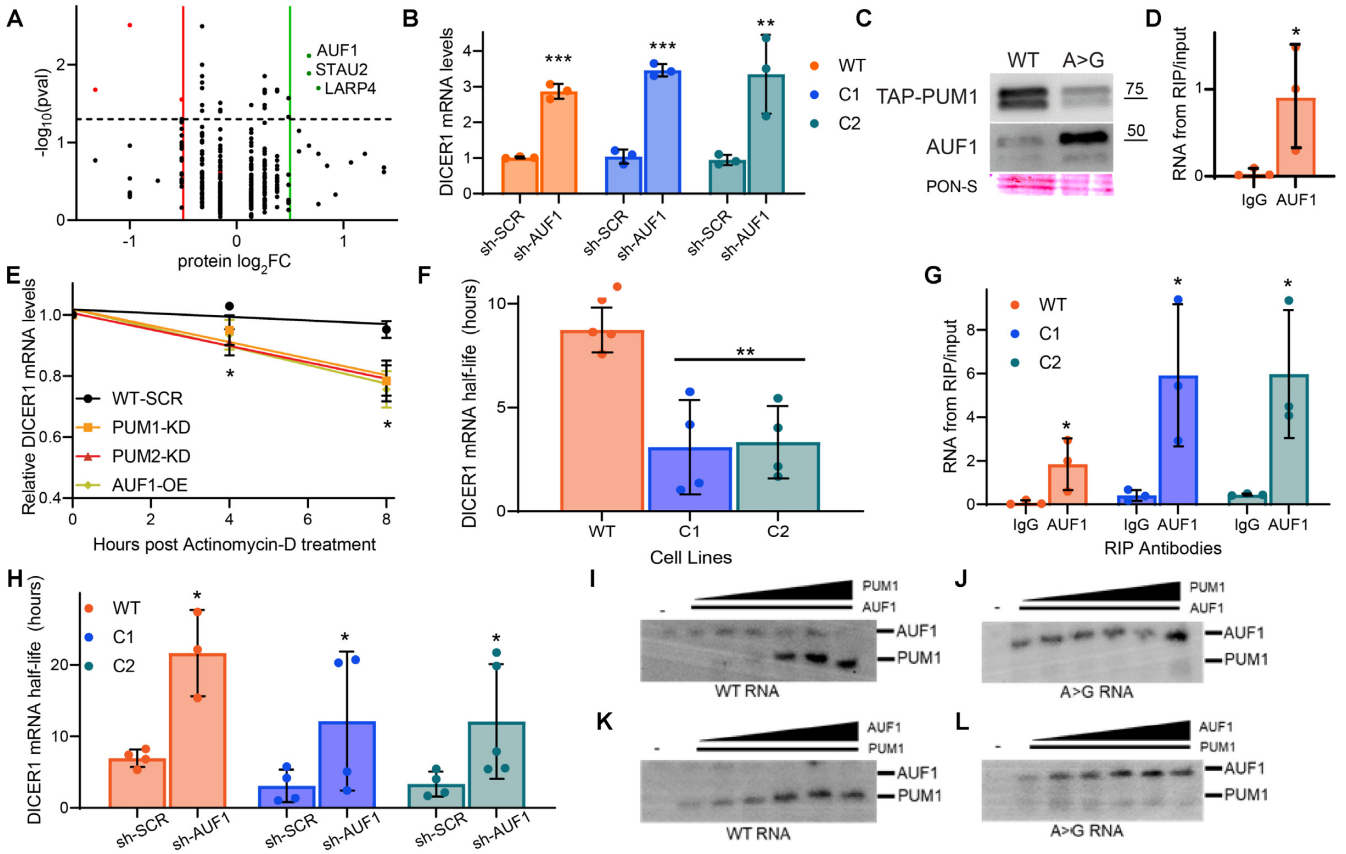

Figure 4. The DICER1 mRNA is destabilized by AUF1 in the absence of PUM-mediated regulation. (**A**) Volcano plot of $\log_2$ (Fold Change) of endogenous RBPs from *in vitro* RNA binding-LC/MS analysis of proteins bound to the DICER1-3′UTR A > G RNA sequence relative DICER1-3′UTR WT RNA sequence. Significantly upregulated genes ($\log_2$FC > 1, $P < 0.05$) are shown in green and significantly downregulated genes ($\log_2$FC < 1, $P < 0.05$) are shown in red. (**B**) DICER1 mRNA levels in WT, C1 and C2 MDA-MB-231 cells depleted of AUF1 or SCR (control) by shRNA. (**C**) PUM1 and AUF1 *in vitro* RNA binding assays of the DICER1 WT and pMUT sequences. (**D**) Relative binding of the DICER1 RNA from RIP-qPCR analysis of IgG (non-specific antibody) and AUF1 in MDA-MB-231 cells. (**E**) Relative DICER1 RNA half-life in MDA-MB-231 cells depleted of SCR, PUM1, PUM2 or over-expressing AUF1. (**F**) RNA half-life of DICER1 mRNA in WT, C1 and C2 MDA-MB-231 cells. (**G**) Relative binding of the DICER1 RNA from RIP-qPCR analysis of IgG (non-specific antibody) and AUF1 in WT, C1 and C2 MDA-MB-231 cells. (**H**) RNA half-life of DICER1 mRNA in WT, C1 and C2 MDA-MB-231 cells depleted with shRNAs targeting control, SCR, or AUF1. (**I**) EMSA from WT DICER1 pre-coated with AUF1 followed by increasing amounts of PUM1. (**J**) EMSA from A > G DICER1 pre-coated with AUF1 followed by increasing amounts of PUM1. (**K**) EMSA from WT DICER1 pre-coated with PUM1 followed by increasing amounts of AUF1. (**L**) EMSA from A > G DICER1 pre-coated with PUM1 followed by increasing amounts of AUF1. $n = 3$, error bar represents standard deviation. *$P < 0.05$, **$P < 0.01$.

PUM1 and AUF1 and found high levels of PUM1 bound to the WT DICER1 RNA, with lower levels of AUF1 interaction (Figure 4C). In contrast, the switch of a single base pair (*rs1252940486*) is sufficient to almost abolish PUM1 binding and promote AUF1 recruitment (A > G) (Figure 4C). By conducting RIP-RT-PCR from MDA-MB-231 cells, we found an endogenous interaction between AUF1 and the DICER1 RNA (Figure 4D). As we have previously found that PUM silencing reduced the overall RNA levels of DICER1 (Figure 2E), we reasoned that if AUF1 was responsible for these changes that its over-expression should mirror PUM-depletion. We treated MDA-MB-231 cells with shRNAs to deplete Scr, PUM1, PUM2 or over-expressed AUF1 before treating cells with the RNA Polymerase inhibitor, Actinomycin D. Silencing of either PUM or the elevated levels of AUF1, reduce DICER1 RNA levels (Figure 4E). This data suggests that PUM and AUF1 regulate DICER1 levels.

To determine how the disruption of the PRE within DICER1 affects DICER1 RNA half-life, we used RNA metabolic labelling and RT-PCR. We found significant reductions in the half-life of the DICER1 RNA in C1 and C2 cells (Figure 4F), relative to WT and housekeeping genes. To assay whether these changes in RNA half-life were due to AUF1 binding, we conducted AUF1 RIP-qPCR analysis from WT, C1 and C2 cells and found elevated AUF1 bound to the DICER1 3′UTR in C1 and C2 cells (Figure 4G), relative to WT. As AUF1 has previously been shown to destabilize its RNA substrates (107), we next assayed, how depleting AUF1 changed the stability of the *DICER1* mRNA in WT, C1 and C2 cell lines. AUF1 silencing significantly rescued DICER1 RNA stability in C1 and C2 cells (Figure 4H). In addition, AUF1-depletion also increased DICER1 half-life in WT cells, suggesting AUF1 is an important regulator of DICER1 RNA (Figure 4H).

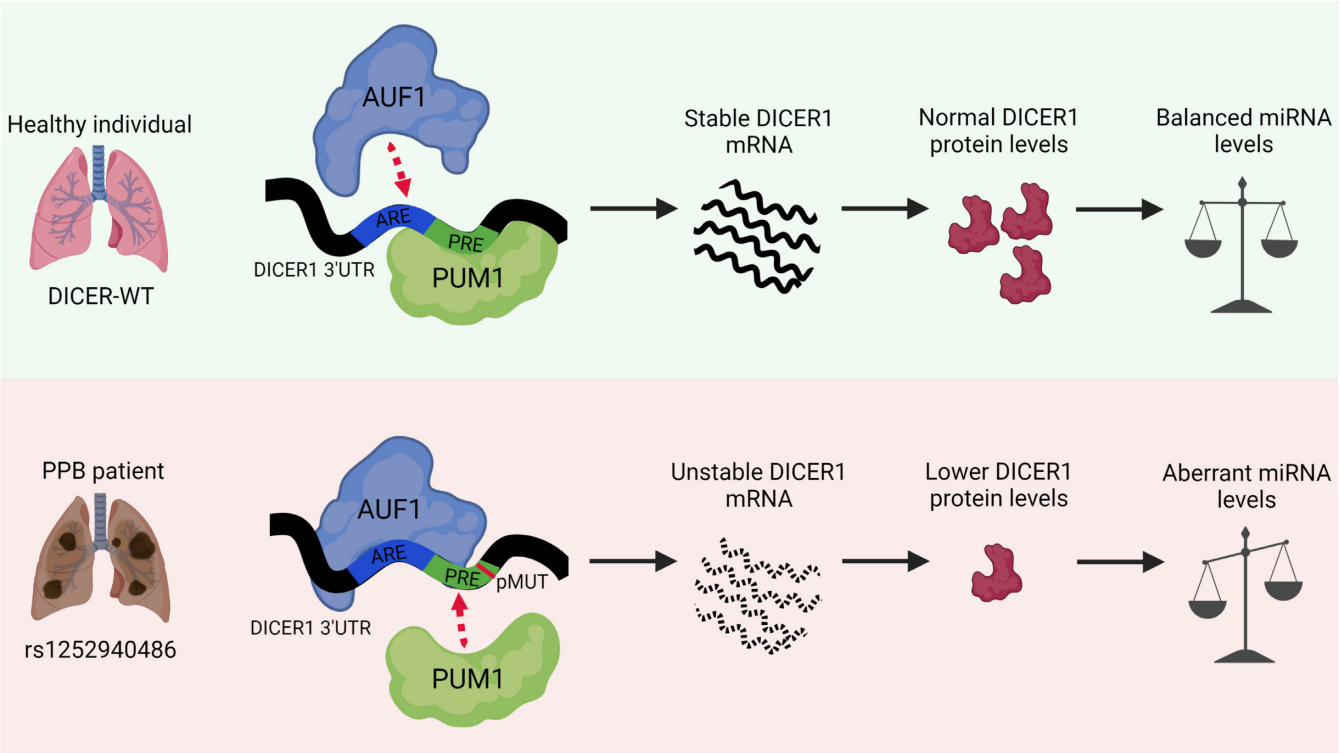

Figure 5. Schematic representation of the post-transcriptional mechanisms regulating DICER1 and their cellular consequence in wildtype and *rs1252940486* 3′UTRs. (**A**) In healthy individuals, with a WT DICER1 3′UTR, the PUM proteins bind with high affinity to the PRE within the 3′UTR and exclude AUF1. This sustains DICER1 mRNA levels and results in normal amounts of DICER1 protein production, miRNA processes and cellular function. In PPB patients with the *rs1252940486* allele, the A > G point mutation alters the PRE motif, which diminishes or destabilizes PUM binding. This enables AUF1 to bind this region and trigger the destabilization of the DICER1 mRNA that results in reduced DICER1 protein and miRNA levels and cellular reprogramming.

PUM1 and AUF1 actively compete to bind the DICER1 3′UTR

PUM and AUF1 both contribute to the overall RNA levels and RNA stability of the DICER1 RNA. To measure the hierarchy of these interactions, we expressed and purified 6xHIS-AUF1 and PUM1 RNA binding domain in *Escherichia coli* (Supplementary Figure S6A/B) and used these proteins for electrophoretic mobility shift assays (EMSA). To examine the competition between AUF1 and PUM1, we pre-coated the WT DICER1 3′UTR RNA with AUF1, and added increasing amounts of PUM1. We found that PUM1 is able to displace AUF1 from the WT RNA (Figure 4I). We next repeated this experiment on the A > G DICER1 3′UTR RNA, and found that PUM1 could not compete with AUF1 binding at any concentration, and that AUF1 remained bound to the RNA (Figure 4J). This suggested that PUM1 binds to the WT DICER1 RNA with higher affinity than AUF1. We next determined whether AUF1 could displace from PUM1 from DICER1 RNA. We pre-coated WT DICER1 RNA with PUM1, and added increasing amounts of AUF1. We found that even at very high concentration, AUF1 can not displace PUM1 from the WT DICER1 RNA (Figure 4K). In contrast, on the A > G DICER1 RNA, PUM1 binding was undetectable, and AUF1 bound even at the lowest concentration (Figure 4L). Collectively, these findings suggest that the PUM proteins and AUF1 actively compete to bind and regulate the DICER1 mRNA. The strong PUM Regulatory Element located close to the polyadenylation signal enables dominant PUM binding and the correct fate for the DICER1 mRNA. Mutations that disrupt this interaction, expose this region to additional RBPs, including AUF1, which triggers RNA degradation, diminished DICER1 protein production and miRNA levels.

DISCUSSION

In this study, we have identified a novel post-transcriptional mechanism that controls the stability of the *DICER1* mRNA. We found that the PUM and AUF1 RBPs actively compete for binding to the DICER1 3′UTR and that mutations that alter this interaction enable elevated AUF1 binding and RNA degradation. This regulation is important as mutations from DICER1 patients, change the hierarchy of PUM and AUF1 binding, resulting in low levels of DICER1 protein and altered miRNA production.

Previous studies that have identified mutations in DICER1 syndrome patient cohorts have focused on mapping mutations in the *DICER1* coding sequences (46) and have provided important insights into the amino acids that enable DICER1 enzymatic activity (108). In contrast, little is known about how mutations within the 3′UTR regions alter the post-transcriptional regulation of *DICER1* and contribute to DICER1 syndrome. A number of studies have investigated the transcriptional regulators of DICER1 and

identified SOX4, MITF, p53 and p63 in different cellular contexts (109–111). The study of the post-transcriptional regulation of the *DICER1* mRNA has primarily focused on its binding and regulation through miRNAs (112–116). The *DICER1* gene contains a large 3′UTR, ∼4 kb, relative to the average human 3′UTR, ∼950 bp (117), suggesting that post-transcriptional regulation may be important for controlling DICER1 levels. Our analysis focused on the role of the human PUM proteins in regulating the mRNA and protein levels of *DICER1*. DICER1 protein and the miRNA levels that they regulate, are tightly controlled in all biological settings, as alterations trigger molecular reprogramming (118), phenotypic changes (119) and affect organismal fitness (120). In addition, DICER1 levels must be tightly constrained to prevent oncogenic transformation, highlighting the significance of understanding the mechanisms regulating DICER1 (121). Here, we utilize mutations from a DICER1 syndrome patient to identify a new and important post-transcriptional regulation of *DICER1*.

In contrast to many PUM-regulated RNAs, we found that PUM-mediated regulation of *DICER1* mRNA is required to sustain DICER1 RNA levels (122). Our data shows that loss of PUM binding to *DICER1*, results in diminished *DICER1* mRNA half-life, protein, and mature miRNAs levels. We found that the PUM proteins have dual roles in modulating DICER1 levels. First, they bind directly to the DICER1 mRNA and regulate its stability and second, their occupancy of the distal 3′UTR limits the access of additional RBPs to this region. This results in a tight correlation between PUM and DICER1 levels, and is important for the correct regulation of the *DICER1* RNA, and subsequent protein levels. Although PUM is generally considered a post-transcriptional repressor, PUM has been shown to bind to and promote the levels of FOXP1, via an analogous mechanism (76). High throughput RBP binding profiles and RNA stability maps, have identified at least 50 transcripts that are bound by the PUM proteins and have decreased RNA levels following PUM depletion (122). These observations show that PUM regulation is highly substrate and context dependent and is likely influenced by complex interactions between mRNAs, RBPs and miRNAs within the matrix of the post-transcriptional network.

Here, we investigated the molecular mechanism affecting DICER1 levels in the absence of PUM-regulation. These experiments determined the interplay and competition between different post-transcriptional regulators of *DICER1* and tested how each contributed to molecular phenotypes. We found that a single nucleotide change in the 3′UTR of DICER1 can have significant effects on DICER1 RNA and protein levels and the subsequent processing of miRNAs by modifying the landscape of RBPs bound to this region. In agreement with studies of *DICER1*$^{-/-}$ human cells (105), we find that changes in DICER1 levels changes the spectrum of mature miRNAs and we find both increased and reduced miRNAs in cells with diminished DICER1 protein levels. This is likely due to widespread miRNA reprogramming following DICER1 protein changes, and we note that highly abundant miRNAs are over-represented in the down-regulated group. Conversely, low abundant miRNAs and those that can be processed by alternate mechanisms are over-represented in the up-regulated miRNA fraction. In our experiment system, where DICER1 protein is still produced, although at reduced levels, our findings closely mirror those from *DICER1*$^{-/-}$ human cells.

Utilizing wild-type and A > G RNA baits, we found three RBPs enriched on the A > G RNA, AUF1, STAU2 and LARP4, only the AUF1 RBP was found to regulate *DICER1* RNA and protein levels. These findings suggest that the presence or absence of a single RBP can alter the local RNA environment of the 3′UTR and that this can have major consequences for the RNA fate and cell physiology. Post-transcriptional regulation occurs in a co-operative manner and the loss of PUM binding, provides opportunities for additional factors to bind and regulate the RNA.

In contrast to the highly sequence-specific PUM proteins, AUF1 is a generic RNA binding protein with an affinity for AU-rich elements (107,123–125). AUF1 destabilizes its substrates RNA instability and has been previously found to bind the *DICER1* mRNA (126). While we and others found that AUF1 is a regulator of *DICER1* RNA levels in cells, this effect is significantly elevated in cells with mutations that prevent PUM binding to the *DICER1* mRNA. Our work supports these findings and shows that AUF1 does bind and regulate DICER1 mRNA levels in cells (with active PUM), as depletion of AUF1 can increase the overall stability and half-life of the DICER1 RNA. In the absence of PUM interaction, AUF1 binding is increased and can oligomerize along the 3′UTR up to the poly-adenylation site, and promote de-adenylation of the mRNA (127,128). These data suggest that in the absence of PUM recruitment, AUF1 becomes the dominant regulator of *DICER1* mRNA fate. Supporting this, we found elevated AUF1 binding to *DICER1* mRNA in cells with PRE mutations and show that AUF1 depletion in these cells, also rescues the decrease in *DICER1* RNA stability. Collectively, our data shows that a number of RBPs actively compete to bind and regulate the 3′ end of the *DICER1* mRNA and that this is important for tightly regulating DICER1 level.

Changes in DICER1 regulation and protein levels, significantly alter the production of mature miRNAs that act as key post-transcriptional rheostats resulting the reprogramming of molecular circuits and cellular and oncogenic processes. Based on these results, our data shows that the *rs1252940486* mutation significantly limits DICER1 production from this allele, mirroring the effects mutations that seen in other DICER1 syndrome patients (50) (Figure 5). Our study highlights the utility of studying mutations in conserved regions in the 3′UTR sequences of rare alleles in human pathologies to uncover important post-transcriptional mechanisms key for regulating biological processes.

DATA AVAILABILITY

The raw miRNA-Seq data is deposited on SRA (BioProject ID: PRJNA770353). The raw proteomics data is deposited on MassIVE proteomics repository (https://doi.org/doi:10.25345/C5F47GZ2W).

SUPPLEMENTARY DATA

Supplementary Data are available at NAR Online.

ACKNOWLEDGEMENTS

We would like to thank the Kathleen Dotts, Kayla Vorhees, Reena Shakya and Liwen Zhang for their technical assistance with this project.

Author contributions: S.R. conducted the experiments throughout this paper. S.R.C., S.J.B. and J.A.W. generated the CRISPR knock-in cells. E.K. produced protein in *E. coli* and conducted the EMSA. J.K.S. conducted the bioinformatics analysis of the miRNA-Seq, exomics and mass spectrometry. M.K. conducted the Cy3-RNA/PUM co-localization experiment. D.F.G. conducted *in vitro* bindings assays. C.L. did the ChIP-Rt-qPCR. D.L.M. and A.L.M. conducted and analyzed the single cell migration data. A.P.G. and W.O.M. conducted the project and wrote the manuscript.

FUNDING

National Cancer Institute [R01 CA251753-01 to W.O.M.]; American Cancer Society Research Scholar Award [RSG-20-060-01-RMC to W.O.M., RSG-21-066-01-CCG to A.M.]; BBSRC [BB/K009393/1 to A.P.G.]; Royal Society Wolfson Research Merit Award [WM170036 to A.P.G]; D.G. received a scholarship from CNPq Science without borders program [245392/2012-2]; NCI [P30 CA016058 to O.S.U.]. Funding for open access charge: O.S.U. University Start up.

Conflict of interest statement. None declared.

REFERENCES

1. Bernstein,E., Caudy,A.A., Hammond,S.M. and Hannon,G.J. (2001) Role for a bidentate ribonuclease in the initiation step of RNA interference. *Nature*, **409**, 363–366.
2. Jaskiewicz,L. and Filipowicz,W. (2008) Role of dicer in posttranscriptional RNA silencing. *Curr. Top. Microbiol. Immunol.*, **320**, 77–97.
3. Vermeulen,A., Behlen,L., Reynolds,A., Wolfson,A., Marshall,W.S., Karpilow,J. and Khvorova,A. (2005) The contributions of dsRNA structure to dicer specificity and efficiency. *RNA*, **11**, 674–682.
4. Maniataki,E. and Mourelatos,Z. (2005) A human, ATP-independent, RISC assembly machine fueled by pre-miRNA. *Genes Dev.*, **19**, 2979–2990.
5. MacRae,I.J., Zhou,K., Li,F., Repic,A., Brooks,A.N., Cande,W.Z., Adams,P.D. and Doudna,J.A. (2006) Structural basis for double-stranded RNA processing by dicer. *Science*, **311**, 195–198.
6. Ting,A.H., Schuebel,K.E., Herman,J.G. and Baylin,S.B. (2005) Short double-stranded RNA induces transcriptional gene silencing in human cancer cells in the absence of DNA methylation. *Nat. Genet.*, **37**, 906–910.
7. Agranat-Tamir,L., Shomron,N., Sperling,J. and Sperling,R. (2014) Interplay between pre-mRNA splicing and microRNA biogenesis within the supraspliceosome. *Nucleic Acids Res.*, **42**, 4640–4651.
8. Friedman,R.C., Farh,K.K.-H., Burge,C.B. and Bartel,D.P. (2008) Most mammalian mRNAs are conserved targets of microRNAs. *Genome Res.*, **19**, 92–105.
9. Rana,T.M. (2007) Illuminating the silence: understanding the structure and function of small RNAs. *Nat. Rev. Mol. Cell Biol.*, **8**, 23–36.
10. Kloosterman,W.P. and Plasterk,R.H.A. (2006) The diverse functions of micrornas in animal development and disease. *Dev. Cell*, **11**, 441–450.
11. Hammond,S.M., Bernstein,E., Beach,D. and Hannon,G.J. (2000) An RNA-directed nuclease mediates post-transcriptional gene silencing in drosophila cells. *Nature*, **404**, 293–296.
12. Gebert,L.F.R. and MacRae,I.J. (2019) Regulation of microRNA function in animals. *Nat. Rev. Mol. Cell Biol.*, **20**, 21–37.
13. Hutvágner,G. and Zamore,P.D. (2002) A microRNA in a multiple-turnover RNAi enzyme complex. *Science*, **297**, 2056–2060.
14. Bartel,D.P. (2018) Metazoan MicroRNAs. Cell, **173**, 20–51.
15. Lee,R.C., Feinbaum,R.L. and Ambros,V. (1993) The c. elegans heterochronic gene lin-4 encodes small RNAs with antisense complementarity to lin-14. *Cell*, **75**, 843–854.
16. Cottrell,K.A., Szczesny,P. and Djuranovic,S. (2017) Translation efficiency is a determinant of the magnitude of miRNA-mediated repression. *Sci. Rep.*, **7**, 14884.
17. Esquela-Kerscher,A. and Slack,F.J. (2006) Oncomirs — microRNAs with a role in cancer. *Nat. Rev. Cancer*, **6**, 259–269.
18. Hébert,S.S. and De Strooper,B. (2009) Alterations of the microRNA network cause neurodegenerative disease. *Trends Neurosci.*, **32**, 199–206.
19. Olejniczak,M., Galka,P. and Krzyzosiak,W.J. (2010) Sequence-non-specific effects of RNA interference triggers and microRNA regulators. *Nucleic Acids Res.*, **38**, 1–16.
20. Ventura,A. and Jacks,T. (2009) MicroRNAs and cancer: short RNAs go a long way. *Cell*, **136**, 586–591.
21. Calin,G.A., Sevignani,C., Dumitru,C.D., Hyslop,T., Noch,E., Yendamuri,S., Shimizu,M., Rattan,S., Bullrich,F., Negrini,M. *et al.* (2004) Human microRNA genes are frequently located at fragile sites and genomic regions involved in cancers. *Proc. Natl. Acad. Sci. U.S.A.*, **101**, 2999–3004.
22. Calin,G.A., Dumitru,C.D., Shimizu,M., Bichi,R., Zupo,S., Noch,E., Aldler,H., Rattan,S., Keating,M., Rai,K. *et al.* (2002) Nonlinear partial differential equations and applications: frequent deletions and down-regulation of micro- RNA genes miR15 and miR16 at 13q14 in chronic lymphocytic leukemia. *Proc. Natl. Acad. Sci. U.S.A.*, **99**, 15524–15529.
23. Cimmino,A., Calin,G.A., Fabbri,M., Iorio,M.V., Ferracin,M., Shimizu,M., Wojcik,S.E., Aqeilan,R.I., Zupo,S., Dono,M. *et al.* (2005) miR-15 and miR-16 induce apoptosis by targeting BCL2. *Proc. Natl. Acad. Sci. U.S.A.*, **102**, 13944–13949.
24. Calin,G.A., Ferracin,M., Cimmino,A., Di Leva,G., Shimizu,M., Wojcik,S.E., Iorio,M.V., Visone,R., Sever,N.I., Fabbri,M. *et al.* (2005) A MicroRNA signature associated with prognosis and progression in chronic lymphocytic leukemia. *N. Engl. J. Med.*, **353**, 1793–1801.
25. Michael,M.Z., O' Connor,S.M., van Holst Pellekaan,N.G., Young,G.P. and James,R.J. (2003) Reduced accumulation of specific microRNAs in colorectal neoplasia. *Mol. Cancer Res.*, **1**, 882–891.
26. Johnson,S.M., Grosshans,H., Shingara,J., Byrom,M., Jarvis,R., Cheng,A., Labourier,E., Reinert,K.L., Brown,D. and Slack,F.J. (2005) RAS is regulated by the let-7 MicroRNA family. *Cell*, **120**, 635–647.
27. Dhawan,A., Scott,J.G., Harris,A.L. and Buffa,F.M. (2018) Pan-cancer characterisation of microRNA across cancer hallmarks reveals microRNA-mediated downregulation of tumour suppressors. *Nat. Commun.*, **9**, 5228.
28. Bernstein,E., Kim,S.Y., Carmell,M.A., Murchison,E.P., Alcorn,H., Li,M.Z., Mills,A.A., Elledge,S.J., Anderson,K.V and Hannon,G.J. (2003) Dicer is essential for mouse development. *Nat. Genet.*, **35**, 215–217.
29. Herriges,J.C., Brown,S., Longhurst,M., Ozmore,J., Moeschler,J.B., Janze,A., Meck,J., South,S.T. and Andersen,E.F. (2019) Identification of two 14q32 deletions involving DICER1 associated with the development of DICER1-related tumors. *Eur. J. Med. Genet.*, **62**, 9–14.
30. Kalis,M., Bolmeson,C., Esguerra,J.L.S., Gupta,S., Edlund,A., Tormo-Badia,N., Speidel,D., Holmberg,D., Mayans,S., Khoo,N.K.S. *et al.* (2011) Beta-Cell specific deletion of dicer1 leads to defective insulin secretion and diabetes mellitus. *PLoS One*, **6**, e29166.
31. Kanellopoulou,C., Muljo,S.A., Kung,A.L., Ganesan,S., Drapkin,R., Jenuwein,T., Livingston,D.M. and Rajewsky,K. (2005) Dicer-deficient mouse embryonic stem cells are defective in differentiation and centromeric silencing. *Genes Dev.*, **19**, 489–501.
32. Oikawa,S., Lee,M., Motohashi,N., Maeda,S. and Akimoto,T. (2019) An inducible knockout of dicer in adult mice does not affect endurance exercise-induced muscle adaptation. *Am. J. Physiol.-Cell Physiol.*, **316**, C285–C292.
33. Dorval,V., Smith,P.Y., Delay,C., Calvo,E., Planel,E., Zommer,N., Buée,L. and Hébert,S.S. (2012) Gene network and pathway analysis

of mice with conditional ablation of dicer in post-mitotic neurons. *PLoS One*, **7**, e44060.
34. Teijeiro,V., Yang,D., Majumdar,S., González,F., Rickert,R.W., Xu,C., Koche,R., Verma,N., Lai,E.C. and Huangfu,D. (2018) DICER1 is essential for self-renewal of human embryonic stem cells. *Stem Cell Rep.*, **11**, 616–625.
35. Zhang,B., Chen,H., Zhang,L., Dakhova,O., Zhang,Y., Lewis,M.T., Creighton,C.J., Ittmann,M.M. and Xin,L. (2013) A dosage-dependent pleiotropic role of dicer in prostate cancer growth and metastasis. *Oncogene*, **33**, 3099–3108.
36. Karube,Y., Tanaka,H., Osada,H., Tomida,S., Tatematsu,Y., Yanagisawa,K., Yatabe,Y., Takamizawa,J., Miyoshi,S., Mitsudomi,T. *et al.* (2005) Reduced expression of dicer associated with poor prognosis in lung cancer patients. *Cancer Sci.*, **96**, 111–115.
37. Shu,G., Yang,Z. and Liu,D. (2012) Immunohistochemical study of dicer and drosha expression in the benign and malignant lesions of gallbladder and their clinicopathological significances. *Pathology - Res. Pract.*, **208**, 392–397.
38. Iliou,M.S., da Silva-Diz,V., Carmona,F.J., Ramalho-Carvalho,J., Heyn,H., Villanueva,A., Muñoz,P. and Esteller,M. (2014) Impaired DICER1 function promotes stemness and metastasis in colon cancer. *Oncogene*, **33**, 4003–4015.
39. Faggad,A., Budczies,J., Tchernitsa,O., Darb-Esfahani,S., Sehouli,J., Müller,B.M., Wirtz,R., Chekerov,R., Weichert,W., Sinn,B. *et al.* (2010) Prognostic significance of dicer expression in ovarian cancer-link to global microRNA changes and oestrogen receptor expression. *J. Pathol.*, **220**, 382–391.
40. Caffrey,E., Ingoldsby,H., Wall,D., Webber,M., Dinneen,K., Murillo,L.S., Inderhaug,C., Newell,J., Gupta,S. and Callagy,G. (2013) Prognostic significance of deregulated dicer expression in breast cancer. *PLoS One*, **8**, e83724.
41. Chiosea,S., Jelezcova,E., Chandran,U., Acquafondata,M., McHale,T., Sobol,R.W. and Dhir,R. (2006) Up-regulation of dicer, a component of the MicroRNA machinery, in prostate adenocarcinoma. *Am. J. Pathol.*, **169**, 1812–1820.
42. Sugito,N., Ishiguro,H., Kuwabara,Y., Kimura,M., Mitsui,A., Kurehara,H., Ando,T., Mori,R., Takashima,N., Ogawa,R. *et al.* (2006) RNASEN regulates cell proliferation and affects survival in esophageal cancer patients. *Clin. Cancer Res.*, **12**, 7322–7328.
43. Faber,C., Horst,D., Hlubek,F. and Kirchner,T. (2011) Overexpression of dicer predicts poor survival in colorectal cancer. *Eur. J. Cancer*, **47**, 1414–1419.
44. Shan,W., Sun,C., Zhou,B., Guo,E., Lu,H., Xia,M., Li,K., Weng,D., Lin,X., Meng,L. *et al.* (2016) Role of dicer as a prognostic predictor for survival in cancer patients: a systematic review with a meta-analysis. *Oncotarget*, **7**, 72672–72684.
45. Stewart,D.R., Best,A.F., Williams,G.M., Harney,L.A., Carr,A.G., Harris,A.K., Kratz,C.P., Dehner,L.P., Messinger,Y.H. and Rosenberg,P.S. (2019) Neoplasm risk among individuals with a pathogenic germline variant in DICER1. *J. Clin. Oncol.*, **37**, 668.
46. Hill,D.A., Ivanovich,J., Priest,J.R., Gurnett,C.A., Dehner,L.P., Desruisseau,D., Jarzembowski,J.A., Wikenheiser-Brokamp,K.A., Suarez,B.K., Whelan,A.J. *et al.* (2009) DICER1 mutations in familial pleuropulmonary blastoma. *Science*, **325**, 965.
47. JR,P., J,W., L,S., V,H., WG,W., RL,B., SH,F., I,N., MD,A., A,P. *et al.* (1996) Pleuropulmonary blastoma: a marker for familial disease. *J. Pediatr.*, **128**, 220–224.
48. Chong,A.-S., Nikiforov,Y.E., Condello,V., Wald,A.I., Nikiforova,M.N., Foulkes,W.D. and Rivera,B. (2021) Prevalence and spectrum of DICER1 mutations in Adult-onset thyroid nodules with indeterminate cytology. *J. Clin. Endocrinol. Metab.*, **106**, 968–977.
49. Canfarotta,M., Riba-Wolman,R., Orsey,A.D., Balarezo,F. and Finck,C. (2016) DICER1 syndrome and thyroid disease. *J. Pediatr. Surg. Case Rep.*, **11**, 31–34.
50. Schultz,K.A.P., Williams,G.M., Kamihara,J., Stewart,D.R., Harris,A.K., Bauer,A.J., Turner,J., Shah,R., Schneider,K., Schneider,K.W. *et al.* (2018) Dicer1 and associated conditions: identification of at-risk individuals and recommended surveillance strategies. *Clin. Cancer Res.*, **24**, 2251–2261.
51. Rakheja,D., Chen,K.S., Liu,Y., Shukla,A.A., Schmid,V., Chang,T.-C., Khokhar,S., Wickiser,J.E., Karandikar,N.J., Malter,J.S. *et al.* (2014) Somatic mutations in DROSHA and DICER1 impair microRNA biogenesis through distinct mechanisms in wilms tumours. *Nat. Commun.*, **5**, 4802.
52. Kim,J., Schultz,K.A.P., Hill,D.A. and Stewart,D.R. (2019) The prevalence of germline DICER1 pathogenic variation in cancer populations. *Mol. Genet. Genomic Med.*, **7**. E555.
53. Brenneman,M., Field,A., Yang,J., Williams,G., Doros,L., Rossi,C., Schultz,K.A., Rosenberg,A., Ivanovich,J., Turner,J. *et al.* (2018) Temporal order of RNase IIIb and loss-of-function mutations during development determines phenotype in pleuropulmonary blastoma /*DICER1* syndrome: a unique variant of the two-hit tumor suppression model. *F1000Research*, **4**, 214.
54. Mayr,C. (2019) What are 3′ UTRs doing? *Cold Spring Harb. Perspect. Biol.*, **11**, a034728.
55. Mayr,C. (2017) Regulation by 3′-untranslated regions. *Annu. Rev. Genet.*, **51**, 171–194.
56. Nishanth,M.J. and Simon,B. (2020) Functions, mechanisms and regulation of pumilio/puf family RNA binding proteins: a comprehensive review. *Mol. Biol. Rep.*, **47**, 785–807.
57. Goldstrohm,A.C., Hall,T.M.T. and McKenney,K.M. (2018) Post-transcriptional regulatory functions of mammalian pumilio proteins. *Trends Genet.*, **34**, 972–990.
58. Gerber,A.P., Luschnig,S., Krasnow,M.A., Brown,P.O. and Herschlag,D. (2006) Genome-wide identification of mRNAs associated with the translational regulator PUMILIO in drosophila melanogaster. *Proc. Natl. Acad. Sci. U.S.A.*, **103**, 4487–4492.
59. Galgano,A., Forrer,M., Jaskiewicz,L., Kanitz,A., Zavolan,M. and Gerber,A.P. (2008) Comparative analysis of mRNA targets for human PUF-family proteins suggests extensive interaction with the miRNA regulatory system. *PLoS One*, **3**, e3164.
60. Sternburg,E.L., Estep,J.A., Nguyen,D.K., Li,Y. and Karginov,F.V. (2018) Antagonistic and cooperative AGO2-PUM interactions in regulating mRNAs. *Sci. Rep.*, **8**, 15316.
61. Zamore,P.D., Williamson,J.R. and Lehmann,R. (1997) The pumilio protein binds RNA through a conserved domain that defines a new class of RNA-binding proteins. RNA, **3**, 1421–1433.
62. Hogan,G.J., Brown,P.O., Herschlag,D., Hanson-Smith,V., DeRisi,J. and Johnson,A. (2015) Evolutionary conservation and diversification of puf RNA binding proteins and their mRNA targets. *PLoS Biol.*, **13**, e1002307.
63. Kedde,M., Van Kouwenhove,M., Zwart,W., Oude Vrielink,J.A.F., Elkon,R. and Agami,R. (2010) A Pumilio-induced RNA structure switch in p27- 3′ UTR controls miR-221 and miR-222 accessibility. *Nat. Cell Biol.*, **12**, 1014–1020.
64. Miles,W.O., Tschop,K., Herr,A., Ji,J.-Y. and Dyson,N.J. (2012) Pumilio facilitates miRNA regulation of the E2F3 oncogene. *Genes Dev.*, **26**, 356–368.
65. Morris,A.R., Mukherjee,N. and Keene,J.D. (2008) Ribonomic analysis of human pum1 reveals cis-trans conservation across species despite evolution of diverse mRNA target sets. *Mol. Cell. Biol.*, **28**, 4093–4103.
66. Chen,D., Zheng,W., Lin,A., Uyhazi,K., Zhao,H. and Lin,H. (2012) Pumilio 1 suppresses multiple activators of p53 to safeguard spermatogenesis. *Curr. Biol.*, **22**, 420–425.
67. Spassov,D.S. and Jurecic,R. (2003) Mouse pum1 and pum2 genes, members of the pumilio family of RNA-binding proteins, show differential expression in fetal and adult hematopoietic stem cells and progenitors. *Blood Cells Mol. Dis.*, **30**, 55–69.
68. Silva,I.L.Z., Robert,A.W., Cabo,G.C., Spangenberg,L., Stimamiglio,M.A., Dallagiovanna,B., Gradia,D.F. and Shigunov,P. (2020) Effects of PUMILIO1 and PUMILIO2 knockdown on cardiomyogenic differentiation of human embryonic stem cells culture. *PLoS One*, **15**, e0222373.
69. Zhang,M., Chen,D., Xia,J., Han,W., Cui,X., Neuenkirchen,N., Hermes,G., Sestan,N. and Lin,H. (2017) Post-transcriptional regulation of mouse neurogenesis by pumilio proteins. *Genes Dev.*, **31**, 1354–1369.
70. Leeb,M., Dietmann,S., Paramor,M., Niwa,H. and Smith,A. (2014) Genetic exploration of the exit from self-renewal using haploid embryonic stem cells. *Cell Stem Cell*, **14**, 385–393.
71. García-Rodríguez,L.J., Gay,A.C. and Pon,L.A. (2007) Puf3p, a pumilio family RNA binding protein, localizes to mitochondria and regulates mitochondrial biogenesis and motility in budding yeast. *J. Cell Biol.*, **176**, 197–207.

72. Kopp,F., Elguindy,M.M., Yalvac,M.E., Zhang,H., Chen,B., Gillett,F.A., Lee,S., Sivakumar,S., Yu,H., Xie,Y. *et al.* (2019) PUMILIO hyperactivity drives premature aging of norad-deficient mice. *Elife*, **8**, 42650.
73. Brocard,M., Khasnis,S., Wood,C.D., Shannon-Lowe,C. and West,M.J. (2018) Pumilio directs deadenylation-associated translational repression of the cyclin-dependent kinase 1 activator RGC-32. *Nucleic Acids Res.*, **46**, 3707–3725.
74. Liu,Y., Qu,L., Liu,Y., Roizman,B. and Zhou,G.G. (2017) PUM1 is a biphasic negative regulator of innate immunity genes by suppressing LGP2. *Proc. Natl. Acad. Sci. U.S.A.*, **114**, E6902–E6911.
75. Subasic,D., Stoeger,T., Eisenring,S., Matia-González,A.M., Imig,J., Zheng,X., Xiong,L., Gisler,P., Eberhard,R., Holtackers,R. *et al.* (2016) Post-transcriptional control of executioner caspases by RNA-binding proteins. *Genes Dev.*, **30**, 2213–2225.
76. Naudin,C., Hattabi,A., Michelet,F., Miri-Nezhad,A., Benyoucef,A., Pflumio,F., Guillonneau,F., Fichelson,S., Vigon,I., Dusanter-Fourt,I. *et al.* (2017) PUMILIO/FOXP1 signaling drives expansion of hematopoietic stem/progenitor and leukemia cells. *Blood*, **129**, 2493–2506.
77. Miles,W.O., Korenjak,M., Griffiths,L.M., Dyer,M.A., Provero,P. and Dyson,N.J. (2014) Post-transcriptional gene expression control by NANOS is up-regulated and functionally important in pRb-deficient cells. *EMBO J.*, **33**, 2201–2215.
78. Gennarino,V.A., Singh,R.K., White,J.J., De Maio,A., Han,K., Kim,J.-Y., Jafar-Nejad,P., di Ronza,A., Kang,H., Sayegh,L.S. *et al.* (2015) Pumilio1 haploinsufficiency leads to SCA1-like neurodegeneration by increasing wild-type ataxin1 levels. *Cell*, **160**, 1087–1098.
79. Gennarino,V.A., Palmer,E.E., McDonell,L.M., Wang,L., Adamski,C.J., Koire,A., See,L., Chen,C.-A., Schaaf,C.P., Rosenfeld,J.A. *et al.* (2018) A mild PUM1 mutation is associated with adult-onset ataxia, whereas haploinsufficiency causes developmental delay and seizures. *Cell*, **172**, 924–936.
80. Follwaczny,P., Schieweck,R., Riedemann,T., Demleitner,A., Straub,T., Klemm,A.H., Bilban,M., Sutor,B., Popper,B. and Kiebler,M.A. (2017) Pumilio2-deficient mice show a predisposition for epilepsy. *Dis. Models Mech.*, **10**, 1333–1342.
81. Siemen,H., Colas,D., Heller,H.C., Brüstle,O. and Reijo Pera,R.A. (2011) Pumilio-2 function in the mouse nervous system. *PLoS One*, **6**, e25932.
82. Mak,W., Fang,C., Holden,T., Dratver,M.B. and Lin,H. (2016) An important role of pumilio 1 in regulating the development of the mammalian female germline1. *Biol. Reprod.*, **94**, 134.
83. Blewett,N.H. and Goldstrohm,A.C. (2012) A eukaryotic translation initiation factor 4E-Binding protein promotes mRNA decapping and is required for PUF repression. *Mol. Cell. Biol.*, **32**, 4181–4194.
84. Friend,K., Campbell,Z.T., Cooke,A., Kroll-Conner,P., Wickens,M.P. and Kimble,J. (2012) A conserved PUF-Ago-eEF1A complex attenuates translation elongation. *Nat. Struct. Mol. Biol.*, **19**, 176–183.
85. Van Etten,J., Schagat,T.L., Hrit,J., Weidmann,C.A., Brumbaugh,J., Coon,J.J. and Goldstrohm,A.C. (2012) Human pumilio proteins recruit multiple deadenylases to efficiently repress messenger RNAs. *J. Biol. Chem.*, **287**, 36370–36383.
86. Rigaut,G., Shevchenko,A., Rutz,B., Wilm,M., Mann,M. and Séraphin,B. (1999) A generic protein purification method for protein complex characterization and proteome exploration. *Nat. Biotechnol.*, **17**, 1030–1032.
87. Chen,C., Ridzon,D.A., Broomer,A.J., Zhou,Z., Lee,D.H., Nguyen,J.T., Barbisin,M., Xu,N.L., Mahuvakar,V.R., Andersen,M.R. *et al.* (2005) Real-time quantification of microRNAs by stem-loop RT-PCR. *Nucleic Acids Res.*, **33**, e179.
88. Langmead,B. and Salzberg,S.L. (2012) Fast gapped-read alignment with bowtie 2. *Nat. Methods*, **9**, 357–359.
89. Danecek,P., Bonfield,J.K., Liddle,J., Marshall,J., Ohan,V., Pollard,M.O., Whitwham,A., Keane,T., McCarthy,S.A., Davies,R.M. *et al.* (2021) Twelve years of SAMtools and BCFtools. *Gigascience*, **10**, giab008.
90. Li,H., Handsaker,B., Wysoker,A., Fennell,T., Ruan,J., Homer,N., Marth,G., Abecasis,G., Durbin,R. and Subgroup,1000 Genome Project Data ProcessingSubgroup,1000 Genome Project Data Processing (2009) The sequence alignment/map format and SAMtools. Bioinformatics, **25**, 2078–2079.
91. Koboldt,D.C., Zhang,Q., Larson,D.E., Shen,D., McLellan,M.D., Lin,L., Miller,C.A., Mardis,E.R., Ding,L. and Wilson,R.K. (2012) VarScan 2: somatic mutation and copy number alteration discovery in cancer by exome sequencing. *Genome Res.*, **22**, 568–576.
92. Meena,N., Mathur,P., Medicherla,K. and Suravajhala,P. (2018) A bioinformatics pipeline for whole exome sequencing: overview of the processing and steps from raw data to downstream analysis. *Bio-Protocol*, **8**, 2805.
93. Ingolia,N.T., Brar,G.A., Rouskin,S., McGeachy,A.M. and Weissman,J.S. (2012) The ribosome profiling strategy for monitoring translation in vivo by deep sequencing of ribosome-protected mRNA fragments. *Nat. Protoc.*, **7**, 1534–1550.
94. Chan,P.P. and Lowe,T.M. (2016) GtRNAdb 2.0: an expanded database of transfer RNA genes identified in complete and draft genomes. *Nucleic Acids Res.*, **44**, D184–D149.
95. Dobin,A., Davis,C.A., Schlesinger,F., Drenkow,J., Zaleski,C., Jha,S., Batut,P., Chaisson,M. and Gingeras,T.R. (2013) STAR: ultrafast universal RNA-seq aligner. *Bioinformatics*, **29**, 15–21.
96. Love,M.I., Huber,W. and Anders,S. (2014) Moderated estimation of fold change and dispersion for RNA-seq data with DESeq2. *Genome Biol.*, **15**, 550.
97. Perkins,D.N., Pappin,D.J.C., Creasy,D.M. and Cottrell,J.S. (1999) Probability-based protein identification by searching sequence databases using mass spectrometry data. *ELECTROPHORESIS*, **20**, 3551–3567.
98. Russo,J., Heck,A.M., Wilusz,J. and Wilusz,C.J. (2017) Metabolic labeling and recovery of nascent RNA to accurately quantify mRNA stability. *Methods*, **120**, 39–48.
99. Xu,N., Chen,C.-Y.A. and Shyu,A.-B. (2001) Versatile role for hnRNP d isoforms in the differential regulation of cytoplasmic mRNA turnover. *Mol. Cell. Biol.*, **21**, 6960–6971.
100. Cuadrado,A., Remeseiro,S., Graña,O., Pisano,D.G. and Losada,A. (2015) The contribution of cohesin-SA1 to gene expression and chromatin architecture in two murine tissues. *Nucleic Acids Res.*, **43**, 3056–3067.
101. HafezQorani,S., Lafzi,A., de Bruin,R.G., van Zonneveld,A.J., van der Veer,E.P., Son,Y.A. and Kazan,H. (2016) Modeling the combined effect of RNA-binding proteins and microRNAs in post-transcriptional regulation. *Nucleic Acids Res.*, **44**, e83.
102. Hafner,M., Landthaler,M., Burger,L., Khorshid,M., Hausser,J., Berninger,P., Rothballer,A., Ascano,M., Jungkamp,A.-C., Munschauer,M. *et al.* (2010) Transcriptome-wide identification of RNA-binding protein and microRNA target sites by PAR-CLIP. *Cell*, **141**, 129–141.
103. Lee,S., Kopp,F., Chang,T.-C., Yu,H., Xie,Y., Mendell,J.T., Sataluri,A., Chen,B. and Sivakumar,S. (2016) Noncoding RNA NORAD regulates genomic stability by sequestering PUMILIO proteins. *Cell*, **164**, 69–80.
104. Cummins,J.M., He,Y., Leary,R.J., Pagliarini,R., Diaz,L.A., Sjoblom,T., Barad,O., Bentwich,Z., Szafranska,A.E., Labourier,E. *et al.* (2006) The colorectal microRNAome. *Proc. Natl. Acad. Sci. U.S.A.*, **103**, 3687–3692.
105. Cummins,J.M., He,Y., Leary,R.J., Pagliarini,R., Diaz,L.A., Sjoblom,T., Barad,O., Bentwich,Z., Szafranska,A.E., Labourier,E. *et al.* (2006) The colorectal microRNAome. *Proc. Natl. Acad. Sci. U.S.A.*, **103**, 3687–3692.
106. Lorenz,R., Hofacker,I.L. and Stadler,P.F. (2016) RNA folding with hard and soft constraints. *Algorithms Mol. Biol.*, **11**, 8.
107. Raineri,I., Wegmueller,D., Gross,B., Certa,U. and Moroni,C. (2004) Roles of AUF1 isoforms, HuR and BRF1 in ARE-dependent mRNA turnover studied by RNA interference. *Nucleic Acids Res.*, **32**, 1279–1288.
108. Foulkes,W.D., Priest,J.R. and Duchaine,T.F. (2014) DICER1: mutations, microRNAs and mechanisms. *Nat. Rev. Cancer*, **14**, 662–672.
109. Jafarnejad,S.M., Ardekani,G.S., Ghaffari,M., Martinka,M. and Li,G. (2013) Sox4-mediated dicer expression is critical for suppression of melanoma cell invasion. *Oncogene*, **32**, 2131–2139.
110. Levy,C., Khaled,M., Robinson,K.C., Veguilla,R.A., Chen,P.-H., Yokoyama,S., Makino,E., Lu,J., Larue,L., Beermann,F. *et al.* (2010) Lineage-specific transcriptional regulation of DICER by MITF in melanocytes. *Cell*, **141**, 994–1005.

111. Boominathan,L. (2010) The guardians of the genome (p53, TA-p73, and TA-p63) are regulators of tumor suppressor miRNAs network. *Cancer Metastasis Rev.*, **29**, 613–639.
112. Martello,G., Rosato,A., Ferrari,F., Manfrin,A., Cordenonsi,M., Dupont,S., Enzo,E., Guzzardo,V., Rondina,M., Spruce,T. *et al.* (2010) A MicroRNA targeting dicer for metastasis control. *Cell*, **141**, 1195–1207.
113. Grelier,G., Voirin,N., Ay,A.-S., Cox,D.G., Chabaud,S., Treilleux,I., Léon-Goddard,S., Rimokh,R., Mikaelian,I., Venoux,C. *et al.* (2009) Prognostic value of dicer expression in human breast cancers and association with the mesenchymal phenotype. *Br. J. Cancer*, **101**, 673–683.
114. Hinkal,G.W., Grelier,G., Puisieux,A. and Moyret-Lalle,C. (2011) Complexity in the regulation of dicer expression: dicer variant proteins are differentially expressed in epithelial and mesenchymal breast cancer cells and decreased during EMT. *Br. J. Cancer*, **104**, 387–388.
115. Feinberg-Gorenshtein,G., Guedj,A., Shichrur,K., Jeison,M., Luria,D., Kodman,Y., Ash,S., Feinmesser,M., Edry,L., Shomron,N. *et al.* (2013) miR-192 directly binds and regulates dicer1 expression in neuroblastoma. *PLoS One*, **8**, e78713.
116. Forman,J.J., Legesse-Miller,A. and Coller,H.A. (2008) A search for conserved sequences in coding regions reveals that the let-7 microRNA targets dicer within its coding sequence. *Proc. Natl. Acad. Sci. U.S.A.*, **105**, 14879–14884.
117. Sood,P., Krek,A., Zavolan,M., Macino,G. and Rajewsky,N. (2006) Cell-type-specific signatures of microRNAs on target mRNA expression. *Proc. Natl. Acad. Sci. U.S.A.*, **103**, 2746–2751.
118. Anokye-Danso,F., Trivedi,C.M., Juhr,D., Gupta,M., Cui,Z., Tian,Y., Zhang,Y., Yang,W., Gruber,P.J., Epstein,J.A. *et al.* (2011) Highly efficient miRNA-Mediated reprogramming of mouse and human somatic cells to pluripotency. *Cell Stem Cell*, **8**, 376–388.
119. Kosik,K.S. (2010) Leading edge essay micrornas and cellular phenotypy. *Cell*, **143**, 21–26.
120. DeVeale,B., Swindlehurst-Chan,J. and Blelloch,R. (2021) The roles of microRNAs in mouse development. *Nat. Rev. Genet.*, **22**, 307–323.
121. Meister,G. (2011) Vision: dicer leaps into view. *Nature*, **471**, 308–309.
122. Bohn,J.A., Van Etten,J.L., Schagat,T.L., Bowman,B.M., McEachin,R.C., Freddolino,P.L. and Goldstrohm,A.C. (2017) Identification of diverse target RNAs that are functionally regulated by human pumilio proteins. *Nucleic Acids Res.*, **46**, 362–386.
123. Xu,N., Chen,C.-Y.A. and Shyu,A.-B. (2001) Versatile role for hnRNP d isoforms in the differential regulation of cytoplasmic mRNA turnover. *Mol. Cell. Biol.*, **21**, 6960–6971.
124. Gratacós,F.M. and Brewer,G. (2010) The role of AUF1 in regulated mRNA decay. *Wiley Interdiscipl. Rev.: RNA*, **1**, 457–473.
125. Dominguez,D., Freese,P., Alexis,M.S., Su,A., Hochman,M., Palden,T., Bazile,C., Lambert,N.J., van Nostrand,E.L., Pratt,G.A. *et al.* (2018) Sequence, structure, and context preferences of human RNA binding proteins. *Mol. Cell*, **70**, 854–867.
126. Abdelmohsen,K., Tominaga-Yamanaka,K., Srikantan,S., Yoon,J.-H., Kang,M.-J. and Gorospe,M. (2012) RNA-binding protein AUF1 represses dicer expression. *Nucleic Acids Res.*, **40**, 11531–11544.
127. Mukherjee,D., Gao,M., O'Connor,J.P., Raijmakers,R., Pruijn,G., Lutz,C.S. and Wilusz,J. (2002) The mammalian exosome mediates the efficient degradation of mRNAs that contain AU-rich elements. *EMBO J.*, **21**, 165–174.
128. Chen,C.Y., Gherzi,R., Ong,S.E., Chan,E.L., Raijmakers,R., Pruijn,G.J.M., Stoecklin,G., Moroni,C., Mann,M. and Karin,M. (2001) AU binding proteins recruit the exosome to degrade ARE-containing mRNAs. *Cell*, **107**, 451–464.